

CoMadOut - A Robust Outlier Detection Algorithm based on CoMAD

Andreas Lohrer^{1,2}, Daniyal Kazempour², Maximilian Hünemörder² and Peer Kröger²

¹Ludwig-Maximilians-Universität München, Oettingenstraße 67, München, 80538, Bavaria, Germany.

²Christian-Albrechts-Universität zu Kiel, Christian-Albrechts-Platz 4, Kiel, 24118, Schleswig-Holstein, Germany.

Contributing authors: alo@informatik.uni-kiel.de;
dka@informatik.uni-kiel.de; mah@informatik.uni-kiel.de;
pkro@informatik.uni-kiel.de;

Abstract

Unsupervised learning methods are well established in the area of anomaly detection and achieve state of the art performances on outlier data sets. Outliers play a significant role, since they bear the potential to distort the predictions of a machine learning algorithm on a given data set. Especially among PCA-based methods, outliers have an additional destructive potential regarding the result: they may not only distort the orientation and translation of the principal components, they also make it more complicated to detect outliers. To address this problem, we propose the robust outlier detection algorithm CoMadOut, which satisfies two required properties: (1) being robust towards outliers and (2) detecting them. Our outlier detection method using coMAD-PCA defines dependent on its variant an inlier region with a robust noise margin by measures of in-distribution (ID) and out-of-distribution (OOD). These measures allow distribution based outlier scoring for each principal component, and thus, for an appropriate alignment of the decision boundary between normal and abnormal instances. Experiments comparing CoMadOut with traditional, deep and other comparable robust outlier detection methods showed that the performance of the introduced CoMadOut approach is competitive to well established methods related to average precision (AP), recall and area under the

receiver operating characteristic (AUROC) curve. In summary our approach can be seen as a robust alternative for outlier detection tasks.

Keywords: Anomaly Detection, Outlier Detection, coMAD, PCA, Unsupervised Machine Learning, Robust Statistics.

Mathematics Subject Classification: 68T99 , 68W25 , 62H86 , 62H25 , 62G35

1 Introduction

Anomaly Detection, one of the major fields of unsupervised machine learning, is an integral part of many domains uncovering the deviations of their data generating processes and thus supporting domain experts in their daily work to prevent unwanted scenarios. However, real world data sets are often highly imbalanced due to the rare occurrence of outliers. For predictive methods represent these outliers both obstacle and opportunity at the same time. They can be considered as an obstacle, because they may distort the precision of the machine learning method. On the other hand outliers present an opportunity, since they may reveal irregular or abnormal behaviour and therefore interesting insights. From the aforementioned two aspects, we can derive two properties that an anomaly detection algorithm needs to satisfy, namely (1) to be resilient towards outlying data instances, while at the same time (2) detect them. A preliminary step of many outlier detection approaches is dimensionality reduction. This part is often done by PCA(Jolliffe, 1986), a technique exploring the directions of highest variances within the data. This is achieved by computing the eigenvectors of the covariance matrix (directions) and the corresponding eigenvalues (variances). Such eigenpairs allow a transformation from the original data to principal components in lower dimensional subspace, and therewith the task of dimensionality reduction and others. However, the usage of the covariance matrix can make the standard PCA susceptible towards outliers, which has lead to the creation of robust PCA methods, that minimize the influence of such outliers.(Candès, Li, Ma, & Wright, 2011) In order to achieve resilience or robustness for PCA-based algorithms, we must ensure that the computed principal components and corresponding eigenvalues are barely, or even better not influenced by instances located out of distribution. In particular this means that robustness is achieved if abnormal instances do not skew the orientation and translation of the eigenvectors and do not lead to an increase or decrease of the eigenvalues.

In this work we introduce CoMadOut, an unsupervised outlier detection method, which shows robustness among other techniques due to outlier resistant CoMAD-PCA(Kazempour, Hünemörder, & Seidl, 2019). While Kazempour et al. demonstrate that coMAD (co-median absolute deviation) is potentially robust towards anomalies, it lacks the ability to *detect*

abnormal instances. Therefore, we suggest with this paper a competitive outlier detection approach called CoMadOut which is capable to detect, score and predict outliers.

Since there already exists a plethora of outlier detection methods, we investigate in this work the performance of CoMadOut against a comprehensive selection of state-of-the-art techniques (cf. section 4) covering both traditional and Deep Anomaly Detection methods.

In summary, this work provides the following contributions:

1. We introduce the robust outlier detection algorithm CoMadOut (CMO) that derives margin-based decision boundaries by utilizing the noise-resistant eigenpairs of CoMAD-PCA.
2. To align the decision boundaries, we offer several outlier scoring variants of CoMadOut, summerized as CMO*, which simultaneously consider measures of out-of-distribution (tailedness) in order to adapt the CMO baseline approach to different distributions.
3. We detail, how the proposed CMO* variants can be combined to an ensemble approach for outlier detection (CMOEns).
4. We show how CoMAD can be used for robust outlier detection.
5. We conduct extensive experiments comparing and discussing the performance of our methods against competitors and several real-world datasets.

The remaining work is structured as follows. In section 2, we give an overview of related work. Section 3 introduces our CoMadOut outlier detection method and elaborate several variants of this method. The experiments are presented in section 4, while section 5 concludes the paper.

2 Related Work

In this section, we review the related literature, concerning all approaches intersecting with our approach CoMadOut. Thereby we divide those into three categories: (1) well established traditional outlier detection methods, (2) deep outlier detection methods, and (3) robust estimation and PCA-based methods, where the latter are optimized towards outlier robustness most similar to our proposed method CoMadOut.

2.1 Traditional Methods

The Local Outlier Factor (LOF)(Breunig, Kriegel, Ng, & Sander, 2000) is a density-based outlier detection method. As such it determines if an object is an outlier based on the k NN-neighborhood. Samples which exhibit a significantly lower density in their own local neighborhood compared to the density of other samples and their respective neighborhoods are identified as outliers.

The Isolation Forest (IF)(Liu, Ting, & Zhou, 2012) method is a tree ensemble approach to identify anomalies. The decision trees of that ensemble are initially constructed by randomly selecting a feature and then performing a

random split between its minimum and maximum value recursively. IF is based on the assumption that outliers exhibit a lower occurrence in contrast to "normal" samples making them appear close to the root of a tree with fewer splits necessary.

The One Class SVM (OCSVM)([Crammer & Chechik, 2004](#)) approach separates all samples from the origin by maximizing the distance from a separating hyperplane to the origin. Therefore, kernels can be utilized to transform the samples into a high dimensional and thus better separable space. Consequently, a binary function computes which regions in the original data space exhibit a high density and are therewith labelled with "+1" while all other samples (outliers) are labelled with "-1".

2.2 Deep Outlier Detection Methods

Two prominent neural network architectures that are commonly used for deep anomaly detection are Vanilla Autoencoders (AE), whose low-dimensional codes compete with those of PCA([Hinton & Salakhutdinov, 2006](#)), and Variational Autoencoders (VAE)([An & Cho, 2015](#)). The underlying concept for both is fairly similar. An Encoder is trained to embed each training sample, so that it can be projected into a generally lower dimensional latent space and then reconstructed by a Decoder network. The assumption for anomaly detection is now that if a model is trained well on normal data, samples that are abnormal should be hard to reconstruct with the same network and therefore have a high reconstruction error. A threshold is then used to identify these anomalies. Among the different variations of AE, VAEs are special versions of autoencoders. VAEs first encode the input as distributions over the latent space followed by a sampling of samples from the learned distributions. In essence VAEs fit normal distributions on the data and achieve a separation from abnormal samples.

2.3 Robust Estimation and PCA-based Methods

Within this work PCA (Principal Component Analysis) of [Jolliffe](#) is denoted as standard PCA. It is a well-known technique to find patterns in high dimensional data by analysing the variances within the data. As stated in previous chapters, its outlier-sensitive mean of the calculated covariance matrix makes it sensitive towards outliers and thus it is not ideal for subsequent tasks like outlier detection. Thus, a more robust, mean-free version is required to perform reliably on outlier data sets.

CoMAD-PCA([Kazempour et al., 2019](#)) follows the same goal as Robust PCA and the core idea behind it is intriguingly simple: Instead of computing the eigendecomposition of the covariance matrix, which is highly susceptible to outliers, the computation is performed on a coMAD matrix ([Falk, 1997](#)). Analogously to the covariance matrix, the coMAD matrix represents the median absolute deviation from the median for each dimension and each respective pair of dimensions. Therefore, the coMAD-PCA considers the components with the

highest deviation to the median, while standard PCA captures the deviation to the mean. Since the mean of standard PCA is generally more sensitive to outliers (Kriegel, Kröger, Schubert, & Zimek, 2008), coMAD-PCA should be less sensitive. That has been shown by the initial results of Kazempour et al., who illustrated the robustness of coMAD-PCA towards outliers.

Amongst the methods that also consider robustness is the so called Minimum Covariance Determinant (MCD)(Rousseeuw, 1984). The goal of MCD is to find a subset of samples whose covariance matrix has the minimum determinant. Its location is then the subset’s average, and its variance is the subset’s covariance matrix. Rousseeuw states in addition that this technique can yield suitable results even when 50% of the data are contaminated with outliers.

Since the performance of Empirical Covariance Estimators, like e.g. the performance of the Maximum Likelihood Covariance Estimator (MLE), suffers from distorted eigenvectors when used on data sets with outliers, more robust methods have been developed. They replace the outlier sensitive parts mean and (co)variance by robust alternatives. These alternatives use e.g. the samples of the lowest covariance matrix determinant (MCD) or randomly selected samples (FastMCD)(Rousseeuw & Driessen, 1999)¹ to provide a robust mean and covariance or compute it deterministically (DetMCD)(Hubert, Rousseeuw, & Verdonck, 2010) in order to achieve a robust distance measure and thereby a high breakdown value².

By following the goal of getting robust towards outliers there had been several ideas to achieve this. At this point the role of coMAD for CoMadOut (cf. section 3 - step 1) shows parallels to the Stahel–Donoho outlyingness (SDO) measure(Maronna & Yohai, 1995), which instead uses a weighted mean vector and covariance matrix, and to the comedian approach(Sajesh & Srinivasan, 2012), which computes robust mahalanobis distances and weights them by a χ^2 -distribution-factor to receive a suitable cut-off value instead. Further methods with parallels to the role of coMAD are estimators like LMS (Least Median Squares)(Rousseeuw, 1984) which fits to the minimal median squared distances and the estimator MOMAD (Median of Means Absolute Deviation)(Depersin & Lecué, 2021), which considers the SDO as notion of depth (close to our notion of robust inlierness in section 3.2) while estimating mean values, which are robust to outliers. PCA-MAD(Huang, Jin, Yu, & Li, 2021) also address the issue of outlier sensitivity and non-robustness of mean-based PCA by weighting outlier scores based on outlier-sensitive standard PCA projections but MAD-weighted z-score distances instead of outlier resistant and kurtosis-weighted coMAD-PCA projection distances or median based margins as the variants of our approach CoMadOut do (cf. Fig. 4).

With this brief overview on the literature of state-of-the-art outlier detection methods we differentiated existing methods from our approach. Best to our knowledge there are no other approaches like our CoMadOut baseline (cf.

¹cf. Elliptic Envelope (<https://scikit-learn.org/stable/modules/generated/sklearn.covariance.EllipticEnvelope.html>)

²proportion of outlier samples an estimator can handle before returning a wrong result

section 3 CMO Steps 1-5) using inlier region enhancing coMAD-based orthogonal distance medians as robustness improving noise margins in combination with coMAD-based robust inlier regions to identify, score and predict outliers. Furthermore, there is no approach like our CoMadOut variants CMO* optimizing coMAD-PCA based outlier scores by simultaneously weighting according to variance or tailedness (cf. section 3.6 CMO* Steps 1-3).

3 CoMadOut

With this section we introduce CoMadOut (CMO), an unsupervised robust outlier detection algorithm, which follows the assumption that coMAD-based principal components and a robust measure of in-distribution (ID), median m , as well as measures of out-of-distribution (OOD), kurtosis κ , optimize the alignment of the decision boundary between normal and abnormal instances. Thus we introduce besides the baseline algorithm CMO also its variants CMO*. The following paragraphs provide a step-wise explanation and address similarities and differences between the several CMO variants. An overview is provided by the table of Fig. 1.

The common goal of all CoMadOut variants is to first of all obtain outlier resistant subspace orientations. This is achieved by (1) using coMAD-PCA (Kazempour et al., 2019) with its robust comedian matrix (Falk, 1997) instead of standard PCA with its outlier sensitive covariance matrix (cf. Fig. 2). This allows CoMadOut to utilize the outlier resistant eigenvectors and eigenvalues of coMAD-PCA in order to receive a robust subspace representation (a coordinate system with axes spanned by the coMAD-PCA eigenvectors) and with that the initial region for inliers for the baseline approach CMO. Since noise is often modeled as a weak form of outliers (Aggarwal, 2016), CoMadOut improves its outlier robustness and its false positive rate also by (2) an additional noise margin (NM) based on the median of the euclidean orthogonal distances between the samples and their subspace axes k extending the initially computed inlier region.

In particular CoMadOut can be described by the following steps and variants. All variants have step 1 and 2 in common and get variant-specific from step 3.

| Sect | Step | CoMadOut (CMO) | CMO+ | CMO+k | CMO+e | CMO+ke | CMOEns | Sect |
|------|------|--|---|-------|-------|--------|--------------------|------|
| 3.1 | 1. | CoMAD-PCA | | | | | | 3.6 |
| 3.2 | 2. | Orthogonal projections on CoMAD-Eigenvectors | | | | | | |
| 3.3 | 3. | coMAD-Eigenvector-Inlier-Margins | Outlier Scoring by Out-Of-Distribution measures | | | | | |
| 3.4 | 4. | coMAD-Eigenvector-Noise-Margins | | | | | obtain max. scores | |
| 3.5 | 5. | CoMadOut Outlier Detection | | | | | z-score threshold | |

Fig. 1: Overview of CoMadOut (CMO) variants and steps.

3.1 Step 1 - Computation of CoMAD-PCA Matrix

Let X be a centered matrix with n samples $x \in \{x_1, x_2, \dots, x_n\}$ having d -dimensional feature vectors in $\mathbb{R}^{n \times d}$ and let the coMAD matrix (Falk, 1997) be defined by

$$X = \begin{pmatrix} x_{1,1} & \dots & x_{1,d} \\ \vdots & \ddots & \vdots \\ x_{n,1} & \dots & x_{n,d} \end{pmatrix}, \quad \text{coMAD}(X) = \begin{pmatrix} \text{comad}(A_1, A_1) & \dots & \text{comad}(A_1, A_d) \\ \vdots & \ddots & \vdots \\ \text{comad}(A_d, A_1) & \dots & \text{comad}(A_d, A_d) \end{pmatrix} \quad (1)$$

with A_k being the k -th feature of samples $x_{*,k}$ and with

$$\text{comad}(A_i, A_j) = \text{med}((A_i - \text{med}(A_i))(A_j - \text{med}(A_j))) \quad (2)$$

so that the coMAD matrix acts as counterpart for the covariance matrix in the original PCA and

$$A_i - \text{med}(A_i) = \text{MAD}(A_i) \quad (3)$$

represents the robustness providing subtraction of the median in place of the subtraction of the outlier sensitive mean. On the resulting coMAD matrix we apply coMAD-PCA (Kazempour et al., 2019) in order to utilize its resulting robust eigenpairs to define the selective inlier region for the CMO baseline. Therefore, we consider

$$\text{coMAD}(X) = U \Lambda U^T \quad (4)$$

with eigenvector matrix U and eigenvalue matrix Λ , where those eigenpairs (consisting out of eigenvector and eigenvalue) with the k -largest eigenvalues are used for the definition of the initial inlier region (for CMO baseline) in the next step 2. Since the ideal choice of K for the number of principal components can vary between data sets, we conducted the experiments of our work (cf. section 4) on different percentages of the total number of L possible subspaces (leading to a different number of K but maximal L principal components) for all data sets and averaged the achieved average performances.

3.2 Step 2 - Orthogonal projections on coMAD-Eigenvectors

In the scope of CoMadOut the previously computed eigenpairs are used to calculate the scores of inlierness and outlierness respectively. Therefore, the orthogonal projections of all samples x are computed for each eigenvector (=principal component). The eigenpairs define the direction (k -th eigenvector \vec{u}_k of matrix U) and scale (k -th eigenvalue λ_k of matrix Λ) of the corresponding eigenvectors, which correspond to the subspace axes.

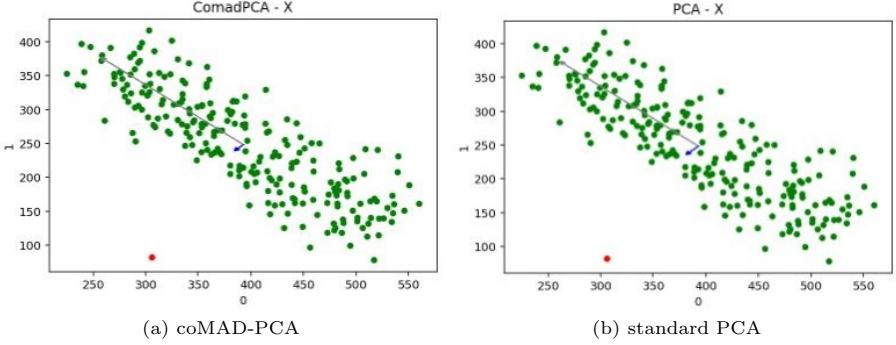


Fig. 2: Illustration of orientation and scale of principal components after applying coMAD-PCA (a) and standard PCA (b) to a synthetic data sets. It can be observed that the outlier (colored in red) has less influence to eigenvectors and eigenvalues of coMAD-PCA on the left than to those of standard PCA on the right.

Formally step 2 can be described by the following equations: $\forall x \in X$ the projections x' can be computed by

$$x' = ((x^T u_k) / (u_k^T u_k)) \cdot u_k \quad (5)$$

Since the origin of the subspace is zero centered after coMAD-PCA from Step 1, the euclidean distances of the projected samples x' to the origin can be computed as

$$x'_k = \sqrt{\sum_{k=1}^K (x'_k)^2} \quad (6)$$

After the first two steps, which have CMO baseline approach and its variants CMO* in common, the next steps are either related to CMO or to its CMO* variants.

3.3 CMO: Step 3 - Computation of coMAD-Eigenvector-Inlier-Margins

The next step for the margin-based CMO baseline approach is to span an initial region for inliers. The eigenpairs define the direction (k -th eigenvector \vec{u}_k of matrix U) and scale (k -th eigenvalue λ_k of matrix Λ) of the corresponding eigenvectors, which correspond to the subspace axes. In order to find out which samples x are part of the inlier region, only samples are considered, which got projected on subspace axis k between its origin O and the absolute length of its axis-corresponding eigenvector \vec{u}_k . Since the eigenvector originally is an unit vector the actual eigenvector length \vec{u}_k - and with that the inlier range for each subspace axis - is defined by the scale of the related eigenvalue λ_k . That

λ_k spans the range of our inlier region in positive and negative eigenvector direction with $[-\lambda_k; +\lambda_k]$ on each subspace axis k .

Formally, the decision for each sample x' , if it lays within the inlier range of all subspace axis eigenvectors \vec{u}_k , is defined as follows:

$$inl(x')_k = \begin{cases} 1, & \text{if } x'_k \in [-\lambda_k; +\lambda_k] \\ 0, & \text{otherwise} \end{cases} \quad (7)$$

In order to avoid inliers to be considered as outliers when the inlier region defining eigenvalue $\lambda_k=0$ a minimum inlier region of $\epsilon=1e-6$ is defined.

In case a sample x' lays within all inlier ranges the product of all subspace-axis- k -related inlier function results

$$inl(x') = \lceil \frac{\sum_{k=1}^K inl(x')_k}{K} \rceil \quad (8)$$

would be equal to 1 (=inlier), otherwise 0 (=non-inlier, cf. section 3.5 step 5).

3.4 CMO: Step 4 - Computation of coMAD-Eigenvector-Noise-Margins

After defining robust inliers in step 3 also noise samples³ are considered for adding them to the set of inliers. Therefore, we enhance the robust inlier region ranges, which are corresponding to their subspace axis k

$$[-\lambda_k; +\lambda_k] \quad (9)$$

by the median of its euclidean orthogonal distances representing our robust noise margin bandwidth $m_k = med(x'_k)$ leading to new inlier region ranges

$$[-m_k - \lambda_k; +\lambda_k + m_k]. \quad (10)$$

Thereby, the restrictive λ -thresholds receive an extended margin for each principal component k , capable to also cover noise samples as inliers by still using the outlier robust distances median instead of the outlier sensitive distances mean.

3.5 CMO: Step 5 - CoMadOut Outlier Detection

Having the final decision boundaries between inliers and outliers available (cf. step 4), this step describes how the CMO baseline approach is able to *identify*, *score* and *predict* samples x as outliers.

Since the coMAD-PCA enables CoMadOut to create its eigenpairs according to the robust coMAD matrix, outliers are less likely to distort their

³in this work samples are considered as noise samples when they are closer to the related subspace axis than its orthogonal distances median m_k but not part of the set of initial robust inliers defined by the coMAD-eigenpairs (cf. section 3.2 step 2)

orientation and scale, which allows to reliably detect inliers in the first phase. Further restrictively selecting noise samples as inliers increases the set of robust inliers and increases thereby the probability that the remaining samples are actual outliers, which as a consequence enables CoMadOut to implicitly identify outliers.

CoMadOut is also capable to provide sample outlier scores sc_i . For this purpose the absolute euclidean distances x'_k of the projected samples x'_i are first reduced by the inlier margin τ_k aiming that actual outlying non-negative distance residuals of the principal components remain. Based on empirical evaluations the best representation for the final outlier score sc_i for a sample x'_i is the mean of its remaining non-negative distance residuals.

$$sc_i = \text{mean}(\max(0, x'_{ik} - \tau_k)) \quad (11)$$

CoMadOut can also provide softmax scores. For that the median from all sample scores sc_i for each score dimension k is calculated to represent an in-distribution score. The non-negative subtraction of that score median from all sample scores allows to uncover residual score dimensions which are more likely to represent an outlier sample so that the subsequent softmax function returns for these dimensions higher outlier scores. The highest softmax score among them represents the softmax score of the related sample x'_i .

$$sc_{i,softmax} = \text{argmax}(\text{softmax}(\frac{\exp(sc_{ik})}{\sum_{j=1}^n \exp(sc_{jk})})) \quad (12)$$

Finally the outlier prediction of the CMO baseline is realized by spanning a parallelogram or parallelepiped volume (for $k=2, 3, \dots, K$ principal components) with the help of the outlier resistant coMAD-eigenpairs according to the related scale (k -th eigenvalue λ_k of matrix Λ) and direction (k -th eigenvector \vec{u}_k of matrix U) respectively, which allows to separate between inliers and outliers by outlier threshold τ with $\tau_k = \lambda_k + m_k$

$$\text{outl}(x')_k = \begin{cases} 1, & \text{if } x'_k \notin [-\tau_k; +\tau_k] \\ 0, & \text{otherwise} \end{cases} \quad (13)$$

In case a sample x' exceeds at least one of the K given subspace axis outlier thresholds τ_k , the outlier decision function

$$\text{outl}(x') = \prod_{k=1}^K \text{outl}(x')_k \quad (14)$$

would be equal to 1 (=outlier) and otherwise 0 (=inlier).

For a geometrical intuition of the scoring and labeling of the CoMadOut baseline approach CMO please see Fig. 3. In Fig. 3 CMO is visualized on a 2-dimensional test data set. The first principal component (PC) is depicted by

the blue and turquoise lines in positive and negative direction and the second PC by the purple and green line accordingly. They define a parallelogram (or parallelepiped volume for $K \geq 3$) for the robust inlier region (light green background) and get extended by the noise margin (NM)(light gray background), which defines the boundary between inliers (green) and outliers (red).

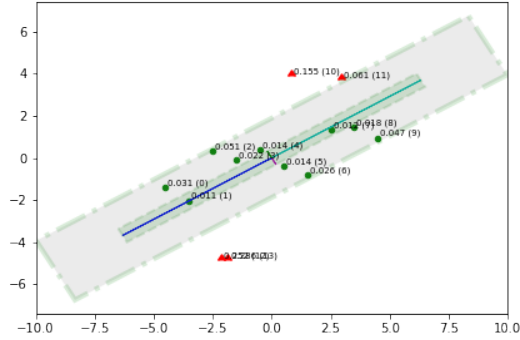


Fig. 3: CoMadOut scoring and labeling of CMO baseline on synthetic data.

3.6 CMO*: Step 3 - Outlier Scoring considering weighting according to out-of-distribution measures

Since the outlier prediction based on the strict inlier and outlier regions of the parallelepiped volume of the CoMadOut baseline approach CMO (cf. Fig. 3) is partially too restrictive for a variety of high-dimensional data sets, further variants of CoMadOut CMO* are introduced with this work. Still utilizing the beneficial properties of coMAD-PCA (cf. sections 3.1 and 3.2 with steps 1 and 2) like outlier resistant eigenpairs or the location of the median as measure of in-distribution, the predictions of variants CMO* are pure outlier scores softening the strict inlier and outlier regions of the CMO baseline.

The related but different approach PCA-MAD of Huang et al. addressed this issue by weighting outlier scores based on outlier-sensitive standard PCA projections (instead of outlier resistant coMAD-PCA projections) and based on principal component based MAD- and median-scaled z-scores.

Our approach CMO+ defines outlier scores based on the sum of absolute distances of coMAD-PCA projections to their zero centered origin O without weighting the outlier scores.

Comparing CMO+ (cf. Fig. 5) and PCA-MAD(Huang et al., 2021) (cf. Fig. 4) one recognizes strong and weak points on both sides. Although the coMAD-based distribution center of CMO+ seems to be well centered and its boundaries are not as geometrically restrictive as those of the CMO baseline it only considers samples quite close to the distribution median as normal.

Depending on the domain-specific anomaly semantics of a data set such outlier scoring could be too restrictive as well. PCA-MAD of [Huang et al.](#) has a broader range of normal non-outlier scores around its MAD-scaled mean but struggles like CMO+ to align its outlier scores close to the distribution boundaries of the longitudinally shaped data set. Scores of border points close to the mean are still representing non-outliers whereas already points in the middle between boundary and mean start to get scored as outliers.

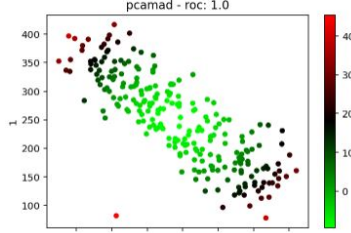


Fig. 4: Outlier score boundaries of competitor PCA-MAD([Huang et al., 2021](#)).

In order to address the issue of neglected distribution boundaries, further CoMadOut variants introduce OOD measures to weight its outlier scores accordingly. CMO+k introduces kurtosis based weighting of outlier scores with

$$SC_{i_{CMO+k}} = \kappa * SC_i \quad (15)$$

with kurtosis κ as a measure of dispersion between the two μ and σ ([Moors, 1986](#)), and provides with that a notion of distribution tailedness.

Formally kurtosis κ is according to Pearson defined as:

$$\kappa = \mathbb{E} \left[\left(\frac{X - \mu}{\sigma} \right)^4 \right] = \frac{\mu^4}{\sigma^4} \quad (16)$$

where μ represents the distribution mean and σ is the standard deviation.

Considering [Fig. 5](#), the kurtosis based weighting of coMAD-PCA based outlier scores sc_i , introduced with CoMadOut variants CMO+k and CMO+ke, contributes to a distribution boundary focused outlier scoring and thus providing a suitable outlier detection algorithm for related data sets and accordingly demanding domains.

Since [Huang et al.](#) demonstrated with λ -weighted distance outlier scores as part of PCA-MAD a comparable positive effect for boundary adapted outlier scoring, its performance is also investigated with the coMAD-based CoMadOut variants CMO+e and CMO+ke where as the latter includes also kurtosis based

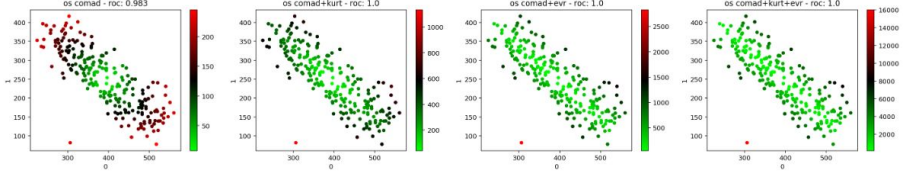


Fig. 5: Outlier score boundaries of CoMadOut variants CMO+, CMO+k, CMO+e, CMO+ke on a synthetic data set (from left to right).

weighting. Formally the outlier scoring of these CoMadOut variants is defined as follows:

$$sc_{i_{CMO+e}} = \frac{sc_i}{\lambda} \quad (17)$$

$$sc_{i_{CMO+ke}} = \frac{\kappa * sc_i}{\lambda} \quad (18)$$

Considering their scoring in Fig. 5 the λ -weighting leads to a permanent notion of normality along the direction of the main principal component so that even boundary points in that direction are considered as normal. Comparing its outlier scoring for boundary points, λ -weighted scoring is related to the variance of the principal components and has thus less focus to the outlier scores of boundary points as the kurtosis weighted outlier scores.

Investigating also in the combined performance of all CoMadOut variants CMO* this work also introduces its ensemble approach CMOEns which standardizes the outlier scores of CMO* methods by its z-score

$$zsc_{i_*} = \frac{sc_{i_*} - \mu_*}{\sigma_*} \quad (19)$$

and selects the largest outlier z-score for each sample among the outlier z-scores of the CMO* approaches.

$$zsc_{i_{CMOEns}} = \max(zsc_{i_{CMO+}}, zsc_{i_{CMO+k}}, zsc_{i_{CMO+e}}, zsc_{i_{CMO+ke}}) \quad (20)$$

For the ensemble variant CMOEns a sample is considered as an outlier when z-score $zsc_{i_{CMOEns}}$ for a sample exceeds the outlier threshold of $z_{thresh} = 1$:

$$outl(zsc_{i_{CMOEns}}) = \begin{cases} 1, & \text{if } zsc_{i_{CMOEns}} \notin [-z_{thresh}; +z_{thresh}] \\ 0, & \text{otherwise} \end{cases} \quad (21)$$

With this section 3 we introduced the CoMadOut variants CMO and CMO* whose performances are investigated in scope of extensive experiments in the next section 4 comparing them to the performance of related and state of the art methods for unsupervised anomaly detection.

4 Experiments

In order to demonstrate the competitiveness of the CoMadOut variants CMO and CMO*, several experiments have been conducted to measure its capability to detect outliers as well as its runtime behavior.

4.1 Setup

For our experiments we used a notebook with Linux Ubuntu 20.04.2 LTS (Focal Fossa), Intel(R) Core(TM) i7-6500U CPU @ 2.50GHz QuadCore and 16GB RAM memory without any usage of GPUs or parallel processing. Moreover, we wrote our experimental code in Python using Jupyter Notebook. The related material will be available on github⁴.

4.1.1 Datasets

First we want to show how data sets could look like on which our CoMadOut approach works well and on which it starts to fail. For this purpose we created a synthetic toy data set shown in Fig. 2 starting with only 1 extreme outlier and 235 instances as part of the main distribution of normal instances we investigate the algorithm robustness in terms of coMAD-PCA based outlier resistance. In order to further extend the experiments with CoMadOut we also benchmarked the variants of our method on *real world data sets* like the well-known Boston Housing Prices⁵ data set, the PARVUS Wine data set⁶ and many other data sets (cf. Table 1) from the ODDS benchmark website⁷ providing more samples and features than the used synthetic data set. For this the Boston Housing Price data set has been enhanced by a ground truth label column "outlier" replacing the original regression value target column "MEDV". Therefore and to receive a preferably linear data set in case of outlier removal, we considered samples laying 2 Inter Quartile Ranges (IQRs) out of the 1st and 3rd quartile as outliers and flagged them with "1" whereas the normal data got flagged with "0". Also the used Wine data set is a specifically tailored version for the task of outlier detection. In this version from ODDS⁶ samples with label "class 1" (cultivator 1) are reduced to 10 samples and flagged as outliers with label "1". Samples with labels "class 2" or "class 3" are considered as normal samples and flagged as inlier with label "0".

4.1.2 Compared Methods

With this paper we also want to benchmark our approach against a wide range of state-of-the-art outlier detection algorithms in order to introduce our method as a further competitive and robust alternative to the already well established outlier detection algorithms and to emphasize the performance of CoMadOut compared to some of its most similar approaches like

⁴<https://github.com/lohrera/CoMadOut>

⁵<https://archive.ics.uci.edu/ml/machine-learning-databases/housing/>

⁶<http://odds.cs.stonybrook.edu/wine-dataset/>

⁷<http://odds.cs.stonybrook.edu>

Table 1: Overview of data sets used in our experiments.

| dataset | samples | features | outliers (percentage) |
|-------------|---------|----------|-----------------------|
| arrhythmia | 451 | 274 | 65 (14.4%) |
| cardio | 1830 | 21 | 176 (9.6%) |
| annthyroid | 7199 | 6 | 534 (7.4%) |
| breastw | 682 | 9 | 239 (35.0%) |
| letter | 1599 | 32 | 100 (6.3%) |
| thyroid | 3771 | 6 | 93 (2.5%) |
| mammography | 11182 | 6 | 260 (2.3%) |
| pima | 767 | 8 | 267 (34.8%) |
| musk | 3061 | 166 | 96 (3.1%) |
| optdigits | 5215 | 64 | 150 (2.9%) |
| pendigits | 6869 | 16 | 156 (2.3%) |
| mnist | 7602 | 100 | 700 (9.2%) |
| shuttle | 49096 | 9 | 3510 (7.1%) |
| satellite | 6434 | 36 | 2036 (31.6%) |
| satimage-2 | 5802 | 36 | 71 (1.2%) |
| wine | 128 | 13 | 9 (7.0%) |
| vowels | 1455 | 12 | 50 (3.4%) |
| glass | 213 | 9 | 9 (4.2%) |
| wbc | 377 | 30 | 21 (5.6%) |
| boston | 506 | 14 | 179 (35.4%) |

PCA-MAD(Huang et al., 2021)⁸, Elliptic Envelope(Rousseeuw & Driessen, 1999)¹ and Minimum Covariance Determinant (MCD)(Rousseeuw, 1984). For the comparison to non- and semi-robust algorithms we also involved several variants of standard PCA methods (PCA from Jolliffe and Shyu, Chen, Sarinapapakorn, and Chang, and standard PCA in combination with the in this work proposed robust noise margin (NM)). In addition to that also traditional outlier detection methods like LOF(Breunig et al., 2000), KNN(Campos et al., 2016), IsolationForest(IF)(Liu et al., 2012), HBOS(Goldstein & Dengel, 2012) and OCSVM(Crammer & Chechik, 2004), as well as modern Deep Outlier Detection methods like AutoEncoder(AE)(Hinton & Salakhutdinov, 2006) and Variational AE(VAE)(An & Cho, 2015) had been involved in our benchmark experiments. As far there existed already reliable implementations of the algorithms in python frameworks like scikit-learn⁹, PyOD¹⁰ or others⁸ then those had been used. Random-states and seed values had been set to 0 for all experiments and hyperparameters had been set as follows for the related data sets (cf. Table 1). CoMadOut (softmax_scoring=False, center_by='median'), PCA-based (n_components=[0.25, 0.4, 0.5, 0.6, 0.75, 0.8, 0.999], AE (hidden_neurons=[4,3,2,2,3,4], batch_size=4, dropout_rate=0.0, epochs=10, l2_regularizer=0.01 for all), VAE (encoder_neurons=[4, 3, 2], decoder_neurons=[2, 3, 4], batch_size=4, epochs=10, dropout_rate=0.0, l2_regularizer=0.001). For all other parameters default values had been used for

⁸<https://github.com/lohrera/pcamad>

⁹<https://scikit-learn.org>

¹⁰<https://pyod.readthedocs.io>

all experiments. So far available, the benchmark results of PCA-MAD(Huang et al., 2021) had been used directly from the paper, otherwise from the non-official implementation⁸. Evaluation metrics described in the subsequent paragraph had been measured with its scikit-learn⁹ implementations.

4.1.3 Evaluation Metrics

Outlier detection can be a semi- or unsupervised task conducting binary decisions whether a given sample is normal (=inlier or noise) or abnormal (=outlier). Since the algorithms are mostly threshold-based and the ratio between normal and abnormal data is more likely to be skewed, we use the evaluation metrics Average Precision (AP), Area Under the Receiver Operating Characteristic (AUROC) curve, Recall and Precision@n ($P@n$) with n equal to the number of total samples. Especially Precision and Recall allow in presence of highly skewed data a more accurate view on an algorithms performance.(Davis & Goadrich, 2006)

4.2 Results

After explaining the experimental setup we introduce our experiment results. The performance of the CoMadOut variants has been compared with that of 20 other outlier detection methods which have been benchmarked with the data sets and evaluation metrics described in section 4.1. Since the performance of the algorithms based on standard PCA and coMAD-PCA is dependent on the number of chosen principal components the benchmark has been run on different percentages (0.25, 0.4, 0.5, 0.6, 0.75, 0.8 and 1.0) of the total number of principal components. In order to demonstrate the differences between the extreme percentages of 0.25 (25%) and 1.0 (100%) both benchmark results are reported for each performance metric starting with the results on all principal components (100%).

The metrics in these tables are representing the performance for each combination between algorithm and data set as well as the average performances ("AVG") of the particular algorithms as well as on a specific data set. The last row "WIN" indicates how many times an algorithm has achieved the best performance from all benchmarked algorithms. The cells highlight the best result per algorithm in green. Results are referenced in brackets related to its paragraph e.g. in paragraph "Results AP & AUROC" the reference (0.416/0.447) means (AP100%: 0.416/AP25%: 0.447).

4.2.1 Results AP & AUROC

Considering the results related to the evaluation metrics AP (cf. Fig. 6 and Fig. 7) CoMadOut variants turn out to win (7/4) datasets out of 20, e.g. CMO+ (0.457/0.453) shows the second best AP average performance behind Isolation Forest (0.47/0.47) and together with CMO+k (0.416/0.447) the best performance among the PCA-based methods.

| dataset | CMO | CMO+ | CMO-k | CMO-e | CMO-ke | CMOEs | PCA-MAD++ | PCA-MAD | HBOS | IF | PCA | PCA(NMI) | LOF | KNN | OC SVM | MCD | EllipticInv | MLE | AE | VAE | AVG |
|--------------|----------|----------|----------|----------|----------|----------|-----------|----------|----------|----------|----------|----------|----------|----------|----------|----------|-------------|----------|----------|----------|----------|
| anrrhythmia | 0.564000 | 0.562000 | 0.399000 | 0.287000 | 0.288000 | 0.276000 | 0.531000 | 0.530000 | 0.450000 | 0.476000 | 0.394000 | 0.505000 | 0.214000 | 0.423000 | 0.351000 | 0.221000 | 0.157000 | 0.285000 | 0.398000 | 0.395000 | 0.385000 |
| cardio | 0.572000 | 0.377000 | 0.266000 | 0.075000 | 0.065000 | 0.128000 | 0.127000 | 0.138000 | 0.443000 | 0.557000 | 0.612000 | 0.112000 | 0.159000 | 0.226000 | 0.137000 | 0.399000 | 0.360000 | 0.464000 | 0.643000 | 0.637000 | 0.337000 |
| anrrhythmoid | 0.596000 | 0.626000 | 0.663000 | 0.635000 | 0.643000 | 0.271000 | 0.547000 | 0.550000 | 0.153000 | 0.258000 | 0.191000 | 0.149000 | 0.082000 | 0.438000 | 0.485000 | 0.505000 | 0.092000 | 0.157000 | 0.195000 | 0.194000 | 0.372000 |
| breastw | 0.893000 | 0.981000 | 0.961000 | 0.967000 | 0.864000 | 0.778000 | 0.919000 | 0.932000 | 0.955000 | 0.963000 | 0.958000 | 0.350000 | 0.275000 | 0.916000 | 0.909000 | 0.697000 | 0.986000 | 0.939000 | 0.768000 | 0.903000 | 0.846000 |
| letter | 0.075000 | 0.082000 | 0.107000 | 0.114000 | 0.116000 | 0.083000 | 0.202000 | 0.083000 | 0.075000 | 0.100000 | 0.076000 | 0.063000 | 0.429000 | 0.306000 | 0.114000 | 0.184000 | 0.184000 | 0.226000 | 0.076000 | 0.079000 | 0.139000 |
| thyroid | 0.790000 | 0.794000 | 0.794000 | 0.773000 | 0.774000 | 0.519000 | 0.784000 | 0.788000 | 0.256000 | 0.524000 | 0.356000 | 0.366000 | 0.050000 | 0.584000 | 0.565000 | 0.702000 | 0.077000 | 0.258000 | 0.407000 | 0.374000 | 0.527000 |
| mammography | 0.032000 | 0.067000 | 0.095000 | 0.048000 | 0.037000 | 0.042000 | 0.069000 | 0.067000 | 0.182000 | 0.169000 | 0.198000 | 0.023000 | 0.110000 | 0.156000 | 0.137000 | 0.042000 | 0.027000 | 0.178000 | 0.198000 | 0.198000 | 0.105000 |
| pima | 0.478000 | 0.500000 | 0.506000 | 0.433000 | 0.400000 | 0.403000 | 0.479000 | 0.477000 | 0.568000 | 0.494000 | 0.467000 | 0.348000 | 0.418000 | 0.528000 | 0.456000 | 0.488000 | 0.488000 | 0.499000 | 0.433000 | 0.395000 | 0.463000 |
| musik | 0.247000 | 0.284000 | 0.225000 | 0.045000 | 0.035000 | 0.092000 | 0.178000 | 0.223000 | 0.992000 | 0.992000 | 1.000000 | 0.212000 | 0.126000 | 0.083000 | 0.120000 | 1.000000 | 0.223000 | 0.499000 | 1.000000 | 1.000000 | 0.444000 |
| optdigits | 0.031000 | 0.047000 | 0.033000 | 0.068000 | 0.061000 | 0.040000 | 0.026000 | 0.028000 | 0.178000 | 0.063000 | 0.027000 | 0.029000 | 0.029000 | 0.024000 | 0.025000 | 0.022000 | 0.029000 | 0.027000 | 0.026000 | 0.027000 | 0.042000 |
| pendigits | 0.246000 | 0.197000 | 0.119000 | 0.018000 | 0.020000 | 0.078000 | 0.147000 | 0.179000 | 0.244000 | 0.236000 | 0.218000 | 0.023000 | 0.042000 | 0.068000 | 0.207000 | 0.069000 | 0.069000 | 0.056000 | 0.221000 | 0.221000 | 0.135000 |
| mnist | 0.096000 | 0.296000 | 0.397000 | 0.200000 | 0.200000 | 0.192000 | 0.082000 | 0.092000 | 0.067000 | 0.231000 | 0.383000 | 0.163000 | 0.129000 | 0.329000 | 0.107000 | 0.309000 | 0.099000 | 0.381000 | 0.386000 | 0.412000 | 0.228000 |
| shuttle | 0.605000 | 0.816000 | 0.141000 | 0.699000 | 0.171000 | 0.801000 | 0.199000 | 0.183000 | 0.957000 | 0.975000 | 0.916000 | 0.120000 | 0.109000 | 0.245000 | 0.599000 | 0.841000 | 0.071000 | 0.871000 | 0.916000 | 0.916000 | 0.570000 |
| satellite | 0.606000 | 0.647000 | 0.665000 | 0.601000 | 0.608000 | 0.551000 | 0.651000 | 0.648000 | 0.662000 | 0.660000 | 0.606000 | 0.316000 | 0.378000 | 0.536000 | 0.640000 | 0.767000 | 0.767000 | 0.514000 | 0.695000 | 0.620000 | 0.607000 |
| satimage-2 | 0.928000 | 0.945000 | 0.972000 | 0.185000 | 0.181000 | 0.074000 | 0.921000 | 0.964000 | 0.755000 | 0.924000 | 0.872000 | 0.012000 | 0.054000 | 0.340000 | 0.954000 | 0.685000 | 0.685000 | 0.367000 | 0.888000 | 0.881000 | 0.628000 |
| wine | 0.564000 | 0.027000 | 0.365000 | 0.073000 | 0.076000 | 0.167000 | 0.240000 | 0.474000 | 0.421000 | 0.211000 | 0.254000 | 0.070000 | 0.314000 | 0.123000 | 0.228000 | 0.678000 | 0.678000 | 0.119000 | 0.097000 | 0.178000 | 0.270000 |
| vowels | 0.063000 | 0.096000 | 0.226000 | 0.055000 | 0.055000 | 0.064000 | 0.278000 | 0.132000 | 0.081000 | 0.155000 | 0.068000 | 0.034000 | 0.281000 | 0.524000 | 0.131000 | 0.055000 | 0.055000 | 0.361000 | 0.064000 | 0.069000 | 0.142000 |
| glass | 0.085000 | 0.083000 | 0.069000 | 0.127000 | 0.111000 | 0.049000 | 0.071000 | 0.077000 | 0.073000 | 0.106000 | 0.071000 | 0.042000 | 0.133000 | 0.141000 | 0.096000 | 0.089000 | 0.089000 | 0.081000 | 0.073000 | 0.080000 | 0.089000 |
| vbc | 0.509000 | 0.483000 | 0.643000 | 0.064000 | 0.037000 | 0.223000 | 0.472000 | 0.540000 | 0.684000 | 0.601000 | 0.557000 | 0.666000 | 0.521000 | 0.482000 | 0.480000 | 0.439000 | 0.439000 | 0.434000 | 0.514000 | 0.525000 | 0.457000 |
| boston | 0.895000 | 0.891000 | 0.883000 | 0.740000 | 0.740000 | 0.567000 | 0.972000 | 0.973000 | 0.583000 | 0.702000 | 0.891000 | 0.365000 | 0.486000 | 0.790000 | 0.954000 | 0.699000 | 0.357000 | 0.590000 | 0.860000 | 0.862000 | 0.748000 |
| AVG | 0.437000 | 0.457000 | 0.416000 | 0.324000 | 0.273000 | 0.269000 | 0.396000 | 0.405000 | 0.440000 | 0.470000 | 0.456000 | 0.198000 | 0.218000 | 0.364000 | 0.394000 | 0.445000 | 0.297000 | 0.385000 | 0.443000 | 0.450000 | 0.000000 |
| WIN | 2.000000 | 2.000000 | 3.000000 | 0.000000 | 0.000000 | 0.000000 | 0.000000 | 1.000000 | 3.000000 | 1.000000 | 2.000000 | 0.000000 | 1.000000 | 2.000000 | 0.000000 | 3.000000 | 2.000000 | 0.000000 | 3.000000 | 3.000000 | 0.000000 |

Fig. 6: Average Precision (AP) performance of 6 CoMadOut (CMO) variants on the left side compared to 14 other anomaly detection algorithms on the right side on 20 real world data sets. The results are based on 100% of all possible principal components.

| dataset | CMO | CMO+ | CMO-k | CMO-e | CMO-ke | CMOEs | PCA-MAD++ | PCA-MAD | HBOS | IF | PCA | PCA(NMI) | LOF | KNN | OC SVM | MCD | EllipticInv | MLE | AE | VAE | AVG |
|--------------|----------|----------|----------|----------|----------|----------|-----------|----------|----------|----------|----------|----------|----------|----------|----------|----------|-------------|----------|----------|----------|----------|
| anrrhythmia | 0.439000 | 0.500000 | 0.508000 | 0.488000 | 0.478000 | 0.260000 | 0.531000 | 0.530000 | 0.450000 | 0.476000 | 0.382000 | 0.377000 | 0.214000 | 0.423000 | 0.351000 | 0.252000 | 0.157000 | 0.286000 | 0.404000 | 0.405000 | 0.396000 |
| cardio | 0.314000 | 0.342000 | 0.380000 | 0.205000 | 0.199000 | 0.150000 | 0.127000 | 0.138000 | 0.443000 | 0.557000 | 0.591000 | 0.115000 | 0.196000 | 0.226000 | 0.133200 | 0.342000 | 0.360000 | 0.464000 | 0.636000 | 0.647000 | 0.338000 |
| anrrhythmoid | 0.346000 | 0.447000 | 0.440000 | 0.438000 | 0.430000 | 0.246000 | 0.575000 | 0.565000 | 0.153000 | 0.258000 | 0.273000 | 0.074000 | 0.082000 | 0.438000 | 0.485000 | 0.505000 | 0.092000 | 0.157000 | 0.194000 | 0.209000 | 0.320000 |
| breastw | 0.805000 | 0.891000 | 0.870000 | 0.843000 | 0.793000 | 0.675000 | 0.905000 | 0.865000 | 0.955000 | 0.963000 | 0.707000 | 0.350000 | 0.275000 | 0.916000 | 0.909000 | 0.697000 | 0.986000 | 0.939000 | 0.768000 | 0.759000 | 0.794000 |
| letter | 0.065000 | 0.060000 | 0.064000 | 0.076000 | 0.066000 | 0.066000 | 0.070000 | 0.070000 | 0.075000 | 0.100000 | 0.077000 | 0.063000 | 0.429000 | 0.306000 | 0.114000 | 0.184000 | 0.184000 | 0.226000 | 0.076000 | 0.077000 | 0.123000 |
| thyroid | 0.816000 | 0.807000 | 0.805000 | 0.802000 | 0.801000 | 0.543000 | 0.789000 | 0.788000 | 0.256000 | 0.524000 | 0.318000 | 0.025000 | 0.050000 | 0.584000 | 0.565000 | 0.702000 | 0.077000 | 0.258000 | 0.407000 | 0.374000 | 0.527000 |
| mammography | 0.023000 | 0.023000 | 0.023000 | 0.027000 | 0.031000 | 0.023000 | 0.016000 | 0.015000 | 0.182000 | 0.169000 | 0.149000 | 0.023000 | 0.110000 | 0.156000 | 0.137000 | 0.045000 | 0.027000 | 0.179000 | 0.197000 | 0.197000 | 0.085000 |
| pima | 0.432000 | 0.462000 | 0.466000 | 0.439000 | 0.447000 | 0.391000 | 0.435000 | 0.438000 | 0.568000 | 0.494000 | 0.379000 | 0.348000 | 0.418000 | 0.528000 | 0.456000 | 0.488000 | 0.488000 | 0.499000 | 0.397000 | 0.481000 | 0.456000 |
| musik | 0.498000 | 0.670000 | 1.000000 | 0.490000 | 0.480000 | 0.164000 | 0.178000 | 0.223000 | 0.992000 | 0.992000 | 0.998000 | 0.199000 | 0.126000 | 0.083000 | 0.120000 | 1.000000 | 0.223000 | 0.499000 | 1.000000 | 1.000000 | 0.550000 |
| optdigits | 0.026000 | 0.039000 | 0.038000 | 0.063000 | 0.071000 | 0.039000 | 0.028000 | 0.027000 | 0.178000 | 0.063000 | 0.025000 | 0.029000 | 0.029000 | 0.024000 | 0.025000 | 0.024000 | 0.029000 | 0.027000 | 0.026000 | 0.029000 | 0.043000 |
| pendigits | 0.592000 | 0.656000 | 0.603000 | 0.522000 | 0.477000 | 0.059000 | 0.135000 | 0.145000 | 0.244000 | 0.236000 | 0.135000 | 0.023000 | 0.042000 | 0.068000 | 0.207000 | 0.069000 | 0.069000 | 0.056000 | 0.268000 | 0.221000 | 0.242000 |
| mnist | 0.089000 | 0.132000 | 0.143000 | 0.197000 | 0.197000 | 0.160000 | 0.230000 | 0.324000 | 0.067000 | 0.231000 | 0.390000 | 0.092000 | 0.129000 | 0.329000 | 0.107000 | 0.256000 | 0.099000 | 0.382000 | 0.386000 | 0.383000 | 0.216000 |
| shuttle | 0.498000 | 0.233000 | 0.077000 | 0.157000 | 0.077000 | 0.073000 | 0.199000 | 0.183000 | 0.957000 | 0.975000 | 0.923000 | 0.071000 | 0.109000 | 0.245000 | 0.599000 | 0.841000 | 0.071000 | 0.871000 | 0.916000 | 0.916000 | 0.450000 |
| satellite | 0.591000 | 0.602000 | 0.618000 | 0.636000 | 0.649000 | 0.515000 | 0.639000 | 0.644000 | 0.682000 | 0.660000 | 0.654000 | 0.316000 | 0.378000 | 0.536000 | 0.640000 | 0.767000 | 0.767000 | 0.514000 | 0.694000 | 0.699000 | 0.610000 |
| satimage-2 | 0.239000 | 0.925000 | 0.963000 | 0.971000 | 0.973000 | 0.076000 | 0.874000 | 0.964000 | 0.755000 | 0.924000 | 0.866000 | 0.012000 | 0.034000 | 0.340000 | 0.954000 | 0.685000 | 0.685000 | 0.367000 | 0.869000 | 0.878000 | 0.666000 |
| wine | 0.576000 | 0.378000 | 0.529000 | 0.495000 | 0.523000 | 0.217000 | 0.460000 | 0.533000 | 0.421000 | 0.211000 | 0.265000 | 0.070000 | 0.314000 | 0.123000 | 0.228000 | 0.678000 | 0.678000 | 0.119000 | 0.097000 | 0.111000 | 0.351000 |
| vowels | 0.031000 | 0.022000 | 0.023000 | 0.026000 | 0.027000 | 0.035000 | 0.021000 | 0.023000 | 0.081000 | 0.155000 | 0.050000 | 0.034000 | 0.281000 | 0.524000 | 0.131000 | 0.055000 | 0.055000 | 0.361000 | 0.059000 | 0.069000 | 0.103000 |
| glass | 0.085000 | 0.080000 | 0.077000 | 0.083000 | 0.080000 | 0.044000 | 0.069000 | 0.079000 | 0.073000 | 0.106000 | 0.076000 | 0.042000 | 0.133000 | 0.141000 | 0.096000 | 0.089000 | 0.089000 | 0.081000 | 0.066000 | 0.069000 | 0.083000 |
| vbc | 0.497000 | 0.525000 | 0.595000 | 0.395000 | 0.475000 | 0.239000 | 0.567000 | 0.543000 | 0.684000 | 0.601000 | 0.502000 | 0.056000 | 0.521000 | 0.482000 | 0.480000 | 0.439000 | 0.439000 | 0.434000 | 0.497000 | 0.533000 | 0.475000 |
| boston | 0.802000 | 0.812000 | 0.701000 | 0.667000 | 0.587000 | 0.507000 | 0.959000 | 0.959000 | 0.959000 | 0.959000 | 0.959000 | 0.959000 | 0.959000 | 0.959000 | 0.959000 | 0.959000 | 0.959000 | 0.959000 | 0.959000 | 0.959000 | 0.959000 |
| AVG | 0.380000 | 0.440000 | 0.440000 | 0.385000 | 0.396000 | 0.224000 | 0.390000 | 0.403000 | 0.440000 | 0.470000 | 0.440000 | 0.134000 | 0.218000 | 0.364000 | 0.394000 | 0.441000 | 0.237000 | 0.385000 | 0.443000 | 0.444000 | 0.300000 |
| WIN | 1.000000 | 1.000000 | 1.000000 | 1.000000 | 1.000000 | 1.000000 | 1.000000 | 1.000000 | 1.000000 | 1.000000 | 1.000000 | 1.000000 | 1.000000 | 1.000000 | 1.000000 | 1.000000 | 1.000000 | 1.000000 | 1.000000 | 1.000000 | 1.000000 |

| dataset | CMO | CMO+ | CMO+k | CMO+e | CMO+ke | CMOEns | PCA-MAD++ | PCA-MAD | HBOS | IF | PCA | PCA(NM) | LOF | KNN | OC SVM | MCD | EllipticEnv | MLE | AE | VAE | AVG |
|-------------|----------|-----------------|-----------------|----------|----------|----------|-----------------|-----------------|-----------------|-----------------|-----------------|----------|-----------------|-----------------|----------|-----------------|-----------------|----------|-----------------|-----------------|----------|
| anthyemia | 0.798000 | 0.633000 | 0.805000 | 0.634000 | 0.655000 | 0.696000 | 0.810000 | 0.813000 | 0.803000 | 0.796000 | 0.775000 | 0.798000 | 0.610000 | 0.797000 | 0.790000 | 0.600000 | 0.508000 | 0.755000 | 0.778000 | 0.775000 | 0.741000 |
| cardio | 0.907000 | 0.900000 | 0.840000 | 0.308000 | 0.275000 | 0.561000 | 0.937000 | 0.955000 | 0.811000 | 0.929000 | 0.950000 | 0.523000 | 0.534000 | 0.742000 | 0.879000 | 0.817000 | 0.816000 | 0.896000 | 0.981000 | 0.955000 | 0.775000 |
| anthyroid | 0.934000 | 0.948000 | 0.959000 | 0.953000 | 0.956000 | 0.634000 | 0.903000 | 0.878000 | 0.606000 | 0.808000 | 0.673000 | 0.541000 | 0.499000 | 0.913000 | 0.936000 | 0.919000 | 0.509000 | 0.641000 | 0.677000 | 0.677000 | 0.776000 |
| breastw | 0.922000 | 0.993000 | 0.985000 | 0.984000 | 0.903000 | 0.845000 | 0.989000 | 0.990000 | 0.985000 | 0.985000 | 0.959000 | 0.500000 | 0.376000 | 0.977000 | 0.952000 | 0.555000 | 0.993000 | 0.972000 | 0.742000 | 0.910000 | 0.876000 |
| letter | 0.330000 | 0.594000 | 0.626000 | 0.688000 | 0.691000 | 0.605000 | 0.659000 | 0.653000 | 0.576000 | 0.670000 | 0.522000 | 0.500000 | 0.686000 | 0.867000 | 0.614000 | 0.810000 | 0.810000 | 0.804000 | 0.515000 | 0.526000 | 0.657000 |
| thyroid | 0.988000 | 0.990000 | 0.990000 | 0.987000 | 0.987000 | 0.862000 | 0.982000 | 0.982000 | 0.935000 | 0.974000 | 0.955000 | 0.682000 | 0.600000 | 0.984000 | 0.986000 | 0.986000 | 0.527000 | 0.934000 | 0.963000 | 0.959000 | 0.913000 |
| mammography | 0.661000 | 0.802000 | 0.840000 | 0.676000 | 0.698000 | 0.647000 | 0.884000 | 0.884000 | 0.856000 | 0.853000 | 0.886000 | 0.500000 | 0.761000 | 0.827000 | 0.827000 | 0.267000 | 0.502000 | 0.866000 | 0.887000 | 0.887000 | 0.748000 |
| pima | 0.680000 | 0.683000 | 0.680000 | 0.609000 | 0.535000 | 0.581000 | 0.713000 | 0.713000 | 0.704000 | 0.666000 | 0.634000 | 0.500000 | 0.611000 | 0.709000 | 0.607000 | 0.681000 | 0.681000 | 0.675000 | 0.596000 | 0.540000 | 0.639000 |
| mus | 0.806000 | 0.887000 | 0.864000 | 0.684000 | 0.592000 | 0.806000 | 1.000000 | 1.000000 | 1.000000 | 1.000000 | 1.000000 | 0.513000 | 0.620000 | 0.477000 | 0.856000 | 0.900000 | 0.599000 | 0.997000 | 1.000000 | 1.000000 | 0.826000 |
| optdigits | 0.551000 | 0.711000 | 0.602000 | 0.723000 | 0.690000 | 0.615000 | 0.717000 | 0.586000 | 0.862000 | 0.765000 | 0.512000 | 0.499000 | 0.484000 | 0.461000 | 0.483000 | 0.416000 | 0.484000 | 0.505000 | 0.507000 | 0.513000 | 0.585000 |
| pendigits | 0.913000 | 0.923000 | 0.886000 | 0.333000 | 0.374000 | 0.851000 | 0.883000 | 0.900000 | 0.924000 | 0.940000 | 0.936000 | 0.500000 | 0.503000 | 0.770000 | 0.930000 | 0.830000 | 0.830000 | 0.763000 | 0.937000 | 0.937000 | 0.794000 |
| mnist | 0.480000 | 0.796000 | 0.847000 | 0.695000 | 0.684000 | 0.757000 | 0.905000 | 0.910000 | 0.370000 | 0.787000 | 0.850000 | 0.701000 | 0.596000 | 0.804000 | 0.605000 | 0.784000 | 0.503000 | 0.846000 | 0.854000 | 0.870000 | 0.732000 |
| shuttle | 0.956000 | 0.920000 | 0.555000 | 0.990000 | 0.734000 | 0.976000 | 0.997000 | 0.998000 | 0.983000 | 0.997000 | 0.990000 | 0.543000 | 0.583000 | 0.760000 | 0.976000 | 0.990000 | 0.500000 | 0.983000 | 0.992000 | 0.990000 | 0.877000 |
| satellite | 0.160000 | 0.656000 | 0.679000 | 0.685000 | 0.690000 | 0.684000 | 0.784000 | 0.783000 | 0.750000 | 0.684000 | 0.601000 | 0.500000 | 0.544000 | 0.676000 | 0.623000 | 0.803000 | 0.803000 | 0.637000 | 0.734000 | 0.612000 | 0.667000 |
| satimage-2 | 0.920000 | 0.998000 | 0.999000 | 0.873000 | 0.883000 | 0.923000 | 0.999000 | 0.999000 | 0.978000 | 0.995000 | 0.977000 | 0.500000 | 0.542000 | 0.926000 | 0.991000 | 0.995000 | 0.995000 | 0.984000 | 0.985000 | 0.986000 | 0.926000 |
| wine | 0.917000 | 0.885000 | 0.932000 | 0.850000 | 0.532000 | 0.767000 | 0.936000 | 0.940000 | 0.916000 | 0.823000 | 0.828000 | 0.500000 | 0.913000 | 0.717000 | 0.820000 | 0.974000 | 0.974000 | 0.691000 | 0.540000 | 0.717000 | 0.791000 |
| vowels | 0.655000 | 0.727000 | 0.826000 | 0.657000 | 0.657000 | 0.701000 | 0.838000 | 0.838000 | 0.676000 | 0.756000 | 0.606000 | 0.500000 | 0.935000 | 0.972000 | 0.714000 | 0.702000 | 0.702000 | 0.912000 | 0.597000 | 0.620000 | 0.730000 |
| glass | 0.735000 | 0.730000 | 0.763000 | 0.817000 | 0.817000 | 0.640000 | 0.746000 | 0.728000 | 0.699000 | 0.742000 | 0.604000 | 0.495000 | 0.806000 | 0.835000 | 0.538000 | 0.771000 | 0.771000 | 0.771000 | 0.532000 | 0.532000 | 0.696000 |
| vbc | 0.927000 | 0.944000 | 0.940000 | 0.290000 | 0.290000 | 0.822000 | 0.936000 | 0.936000 | 0.957000 | 0.944000 | 0.935000 | 0.489000 | 0.942000 | 0.944000 | 0.944000 | 0.917000 | 0.917000 | 0.931000 | 0.896000 | 0.823000 | 0.859000 |
| boaton | 0.974000 | 0.982000 | 0.895000 | 0.811000 | 0.783000 | 0.967000 | 0.976000 | 0.976000 | 0.699000 | 0.825000 | 0.925000 | 0.508000 | 0.681000 | 0.887000 | 0.960000 | 0.757000 | 0.593000 | 0.973000 | 0.930000 | 0.934000 | 0.810000 |
| avg | 0.796000 | 0.649000 | 0.816000 | 0.695000 | 0.665000 | 0.728000 | 0.880000 | 0.874000 | 0.805000 | 0.847000 | 0.806000 | 0.560000 | 0.645000 | 0.803000 | 0.801000 | 0.778000 | 0.697000 | 0.805000 | 0.780000 | 0.800000 | 0.000000 |
| WIN | 0.000000 | 4.000000 | 3.000000 | 0.000000 | 0.000000 | 0.000000 | 3.000000 | 5.000000 | 3.000000 | 2.000000 | 1.000000 | 0.000000 | 1.000000 | 2.000000 | 0.000000 | 3.000000 | 3.000000 | 0.000000 | 3.000000 | 2.000000 | 0.000000 |

Fig. 8: AUROC performance of 6 CoMadOut (CMO) variants on the left side compared to 14 other anomaly detection algorithms on the right side on 20 real world data sets. The results are based on 100% of all possible principal components.

| dataset | CMO | CMO+ | CMO+k | CMO+e | CMO+ke | CMOEns | PCA-MAD++ | PCA-MAD | HBOS | IF | PCA | PCA(NM) | LOF | KNN | OC SVM | MCD | EllipticEnv | MLE | AE | VAE | AVG |
|-------------|----------|----------|----------|----------|----------|----------|-----------|----------|----------|----------|----------|----------|----------|----------|----------|----------|-------------|----------|----------|----------|----------|
| anthyemia | 0.753000 | 0.810000 | 0.819000 | 0.824000 | 0.819000 | 0.620000 | 0.810000 | 0.813000 | 0.803000 | 0.796000 | 0.772000 | 0.705000 | 0.610000 | 0.797000 | 0.790000 | 0.628000 | 0.508000 | 0.756000 | 0.784000 | 0.785000 | 0.750000 |
| cardio | 0.779000 | 0.855000 | 0.864000 | 0.757000 | 0.750000 | 0.648000 | 0.937000 | 0.955000 | 0.811000 | 0.929000 | 0.943000 | 0.529000 | 0.534000 | 0.742000 | 0.879000 | 0.784000 | 0.816000 | 0.896000 | 0.959000 | 0.953000 | 0.816000 |
| anthyroid | 0.877000 | 0.826000 | 0.820000 | 0.818000 | 0.811000 | 0.636000 | 0.903000 | 0.878000 | 0.606000 | 0.808000 | 0.767000 | 0.500000 | 0.459000 | 0.913000 | 0.913000 | 0.919000 | 0.509000 | 0.641000 | 0.677000 | 0.669000 | 0.740000 |
| breastw | 0.829000 | 0.907000 | 0.897000 | 0.864000 | 0.822000 | 0.770000 | 0.989000 | 0.990000 | 0.985000 | 0.985000 | 0.978000 | 0.500000 | 0.376000 | 0.977000 | 0.952000 | 0.555000 | 0.993000 | 0.972000 | 0.741000 | 0.732000 | 0.826000 |
| letter | 0.508000 | 0.485000 | 0.507000 | 0.522000 | 0.543000 | 0.523000 | 0.659000 | 0.653000 | 0.576000 | 0.670000 | 0.503000 | 0.500000 | 0.686000 | 0.867000 | 0.614000 | 0.810000 | 0.810000 | 0.804000 | 0.503000 | 0.525000 | 0.623000 |
| thyroid | 0.993000 | 0.993000 | 0.993000 | 0.993000 | 0.992000 | 0.857000 | 0.982000 | 0.982000 | 0.935000 | 0.974000 | 0.978000 | 0.500000 | 0.600000 | 0.984000 | 0.986000 | 0.986000 | 0.527000 | 0.934000 | 0.968000 | 0.956000 | 0.906000 |
| mammography | 0.481000 | 0.466000 | 0.589000 | 0.538000 | 0.629000 | 0.497000 | 0.884000 | 0.884000 | 0.856000 | 0.853000 | 0.732000 | 0.500000 | 0.761000 | 0.827000 | 0.827000 | 0.267000 | 0.502000 | 0.867000 | 0.886000 | 0.886000 | 0.796000 |
| pima | 0.609000 | 0.623000 | 0.625000 | 0.621000 | 0.625000 | 0.570000 | 0.713000 | 0.713000 | 0.704000 | 0.666000 | 0.522000 | 0.500000 | 0.611000 | 0.709000 | 0.607000 | 0.681000 | 0.681000 | 0.675000 | 0.542000 | 0.654000 | 0.633000 |
| mus | 0.840000 | 0.992000 | 1.000000 | 0.917000 | 0.982000 | 0.917000 | 1.000000 | 1.000000 | 1.000000 | 1.000000 | 1.000000 | 0.519000 | 0.620000 | 0.477000 | 0.856000 | 1.000000 | 0.599000 | 0.997000 | 1.000000 | 1.000000 | 0.897000 |
| optdigits | 0.448000 | 0.659000 | 0.768000 | 0.795000 | 0.812000 | 0.605000 | 0.717000 | 0.586000 | 0.862000 | 0.765000 | 0.470000 | 0.500000 | 0.484000 | 0.461000 | 0.483000 | 0.449000 | 0.494000 | 0.505000 | 0.506000 | 0.549000 | 0.597000 |
| pendigits | 0.955000 | 0.948000 | 0.949000 | 0.871000 | 0.866000 | 0.781000 | 0.862000 | 0.900000 | 0.924000 | 0.948000 | 0.918000 | 0.500000 | 0.503000 | 0.770000 | 0.930000 | 0.830000 | 0.830000 | 0.763000 | 0.940000 | 0.937000 | 0.842000 |
| mnist | 0.525000 | 0.616000 | 0.590000 | 0.720000 | 0.719000 | 0.690000 | 0.905000 | 0.910000 | 0.370000 | 0.787000 | 0.854000 | 0.500000 | 0.596000 | 0.804000 | 0.605000 | 0.755000 | 0.503000 | 0.846000 | 0.854000 | 0.855000 | 0.699000 |
| shuttle | 0.974000 | 0.781000 | 0.514000 | 0.749000 | 0.515000 | 0.503000 | 0.997000 | 0.998000 | 0.983000 | 0.997000 | 0.990000 | 0.500000 | 0.583000 | 0.760000 | 0.976000 | 0.990000 | 0.500000 | 0.983000 | 0.990000 | 0.990000 | 0.805000 |
| satellite | 0.161000 | 0.668000 | 0.629000 | 0.697000 | 0.705000 | 0.680000 | 0.784000 | 0.783000 | 0.750000 | 0.684000 | 0.646000 | 0.500000 | 0.544000 | 0.676000 | 0.623000 | 0.803000 | 0.803000 | 0.637000 | 0.731000 | 0.715000 | 0.688000 |
| satimage-2 | 0.913000 | 0.984000 | 0.997000 | 0.999000 | 0.999000 | 0.925000 | 0.999000 | 0.999000 | 0.978000 | 0.995000 | 0.974000 | 0.500000 | 0.542000 | 0.926000 | 0.991000 | 0.995000 | 0.995000 | 0.984000 | 0.977000 | 0.986000 | 0.934000 |
| wine | 0.963000 | 0.913000 | 0.958000 | 0.850000 | 0.923000 | 0.835000 | 0.936000 | 0.940000 | 0.916000 | 0.823000 | 0.828000 | 0.500000 | 0.913000 | 0.717000 | 0.820000 | 0.974000 | 0.974000 | 0.691000 | 0.539000 | 0.578000 | 0.838000 |
| vowels | 0.378000 | 0.278000 | 0.292000 | 0.355000 | 0.375000 | 0.515000 | 0.838000 | 0.838000 | 0.676000 | 0.756000 | 0.603000 | 0.500000 | 0.935000 | 0.972000 | 0.714000 | 0.702000 | 0.702000 | 0.912000 | 0.574000 | 0.619000 | 0.627000 |
| glass | 0.731000 | 0.737000 | 0.728000 | 0.748000 | 0.739000 | 0.518000 | 0.740000 | 0.728000 | 0.699000 | 0.742000 | 0.570000 | 0.500000 | 0.806000 | 0.835000 | 0.528000 | 0.771000 | 0.771000 | 0.586000 | 0.521000 | 0.578000 | 0.679000 |
| vbc | 0.921000 | 0.942000 | 0.947000 | 0.923000 | 0.931000 | 0.811000 | 0.938000 | 0.938000 | 0.957000 | 0.944000 | 0.896000 | 0.500000 | 0.942000 | 0.944000 | 0.944000 | 0.917000 | 0.910000 | 0.931000 | 0.896000 | 0.914000 | 0.902000 |
| boston | 0.885000 | 0.889000 | 0.791000 | 0.731000 | 0.689000 | 0.667000 | 0.959000 | 0.959000 | 0.699000 | 0.823000 | 0.861000 | 0.500000 | 0.642000 | 0.881000 | 0.881000 | 0.597000 | 0.500000 | 0.734000 | 0.689000 | 0.893000 | 0.784000 |
| AVG | 0.736000 | 0.766000 | 0.764000 | 0.770000 | 0.764000 | 0.676000 | 0.879000 | 0.879000 | 0.805000 | 0.847000 | 0.771000 | 0.516000 | 0.644000 | 0.803000 | 0.801000 | 0.788000 | 0.697000 | 0.805000 | 0.774000 | 0.785000 | 0.000000 |
| WIN | 2.000000 | 1.000000 | 2.000000 | 3.000000 | 1.000000 | 1.000000 | 3.000000 | 3.000000 | 1.000000 | 1.000000 | 1.000000 | 1.000000 | 2.000000 | 2.000000 | 2.000000 | 3.000000 | 1.000000 | 2.000000 | 2.000000 | 2.000000 | 0.000000 |

| dataset | CMO | CMO+ | CMO+k | CMO+e | CMO+ke | CMOEns | PCA-MAD++ | PCA-MAD | HBOS | IF | PCA | PCA(NMI) | LOF | KNN | OC SVM | MCD | EllipticEnv | MLE | AE | VAE | AVG |
|-------------|----------|----------|----------|----------|----------|----------|-----------|----------|----------|----------|----------|----------|----------|----------|----------|----------|-------------|----------|----------|----------|----------|
| arrhythmia | 0.562000 | 0.558900 | 0.391000 | 0.282000 | 0.282000 | 0.497000 | 0.539000 | 0.528000 | 0.443000 | 0.472000 | 0.387000 | 0.503000 | 0.208000 | 0.417000 | 0.343000 | 0.214000 | 0.579000 | 0.277000 | 0.391000 | 0.388000 | 0.413000 |
| cardio | 0.571000 | 0.374000 | 0.264000 | 0.069000 | 0.064000 | 0.268000 | 0.124000 | 0.136000 | 0.441000 | 0.555000 | 0.610000 | 0.178000 | 0.194000 | 0.222000 | 0.329000 | 0.396000 | 0.356000 | 0.462000 | 0.661000 | 0.635000 | 0.345000 |
| anthyroid | 0.595000 | 0.625000 | 0.662000 | 0.635000 | 0.642000 | 0.560000 | 0.546000 | 0.562000 | 0.151000 | 0.256000 | 0.190000 | 0.535000 | 0.081000 | 0.436000 | 0.484000 | 0.504000 | 0.546000 | 0.156000 | 0.193000 | 0.193000 | 0.423000 |
| breastc | 0.908000 | 0.967000 | 0.961000 | 0.967000 | 0.883000 | 0.862000 | 0.919000 | 0.931000 | 0.955000 | 0.963000 | 0.958000 | 0.675000 | 0.274000 | 0.915000 | 0.908000 | 0.871000 | 0.986000 | 0.939000 | 0.768000 | 0.903000 | 0.867000 |
| letter | 0.072000 | 0.073000 | 0.104000 | 0.112000 | 0.113000 | 0.317000 | 0.198000 | 0.082000 | 0.073000 | 0.097000 | 0.072000 | 0.531000 | 0.470000 | 0.301000 | 0.111000 | 0.180000 | 0.180000 | 0.222000 | 0.072000 | 0.075000 | 0.171000 |
| thyroid | 0.789000 | 0.793000 | 0.793000 | 0.771000 | 0.773000 | 0.719000 | 0.782000 | 0.787000 | 0.235000 | 0.521000 | 0.353000 | 0.684000 | 0.047000 | 0.582000 | 0.560000 | 0.700000 | 0.359000 | 0.251000 | 0.404000 | 0.371000 | 0.571000 |
| mammography | 0.033000 | 0.066000 | 0.094000 | 0.048000 | 0.037000 | 0.264000 | 0.088000 | 0.066000 | 0.176000 | 0.160000 | 0.196000 | 0.512000 | 0.113000 | 0.153000 | 0.135000 | 0.035000 | 0.514000 | 0.175000 | 0.195000 | 0.195000 | 0.163000 |
| pinus | 0.476000 | 0.497000 | 0.504000 | 0.429000 | 0.397000 | 0.538000 | 0.478000 | 0.473000 | 0.566000 | 0.491000 | 0.464000 | 0.674000 | 0.415000 | 0.524000 | 0.452000 | 0.486000 | 0.486000 | 0.494000 | 0.423000 | 0.391000 | 0.483000 |
| musk | 0.246000 | 0.283000 | 0.225000 | 0.044000 | 0.034000 | 0.480000 | 0.178000 | 0.223000 | 0.992000 | 0.992000 | 1.000000 | 0.212000 | 0.124000 | 0.081000 | 0.117000 | 1.000000 | 0.612000 | 0.898000 | 1.000000 | 1.000000 | 0.487000 |
| optdigits | 0.030000 | 0.048000 | 0.032000 | 0.066000 | 0.059000 | 0.292000 | 0.026000 | 0.027000 | 0.173000 | 0.061000 | 0.026000 | 0.014000 | 0.028000 | 0.024000 | 0.025000 | 0.022000 | 0.014000 | 0.026000 | 0.036000 | 0.026000 | 0.052000 |
| pendigits | 0.241000 | 0.192000 | 0.117000 | 0.071000 | 0.020000 | 0.518000 | 0.143000 | 0.177000 | 0.239000 | 0.232000 | 0.216000 | 0.511000 | 0.041000 | 0.084000 | 0.204000 | 0.068000 | 0.068000 | 0.055000 | 0.218000 | 0.218000 | 0.179000 |
| mnist | 0.089000 | 0.295000 | 0.396000 | 0.199000 | 0.200000 | 0.526000 | 0.546000 | 0.546000 | 0.067000 | 0.230000 | 0.382000 | 0.165000 | 0.128000 | 0.328000 | 0.106000 | 0.309000 | 0.467000 | 0.083000 | 0.385000 | 0.411000 | 0.308000 |
| shuttle | 0.040000 | 0.615000 | 0.141000 | 0.938000 | 0.171000 | 0.898000 | 0.799000 | 0.183000 | 0.956000 | 0.975000 | 0.915000 | 0.335000 | 0.109000 | 0.245000 | 0.602000 | 0.841000 | 0.253600 | 0.871000 | 0.916000 | 0.915000 | 0.582000 |
| satellite | 0.060000 | 0.047000 | 0.660000 | 0.060000 | 0.068000 | 0.722000 | 0.651000 | 0.646000 | 0.682000 | 0.660000 | 0.606000 | 0.658000 | 0.377000 | 0.536000 | 0.640000 | 0.620000 | 0.767000 | 0.767000 | 0.514000 | 0.695000 | 0.620000 |
| satimage-2 | 0.060000 | 0.944000 | 0.972000 | 0.179000 | 0.171000 | 0.537000 | 0.920000 | 0.964000 | 0.754000 | 0.924000 | 0.872000 | 0.506000 | 0.052000 | 0.336000 | 0.954000 | 0.682000 | 0.682000 | 0.682000 | 0.080000 | 0.881000 | 0.674000 |
| wine | 0.312000 | 0.233000 | 0.320000 | 0.064000 | 0.067000 | 0.494000 | 0.212000 | 0.446000 | 0.365000 | 0.186000 | 0.219000 | 0.535000 | 0.281000 | 0.107000 | 0.198000 | 0.655000 | 0.650000 | 0.103000 | 0.080000 | 0.154000 | 0.284000 |
| vowels | 0.059000 | 0.091000 | 0.218000 | 0.053000 | 0.053000 | 0.394000 | 0.271000 | 0.123000 | 0.074000 | 0.144000 | 0.063000 | 0.517000 | 0.266000 | 0.494000 | 0.119000 | 0.052000 | 0.052000 | 0.347000 | 0.058000 | 0.065000 | 0.176000 |
| glass | 0.072000 | 0.070000 | 0.081000 | 0.062000 | 0.084000 | 0.056000 | 0.021000 | 0.110000 | 0.110000 | 0.110000 | 0.090000 | 0.080000 | 0.080000 | 0.060000 | 0.059000 | 0.080000 | 0.080000 | 0.060000 | 0.059000 | 0.066000 | 0.081000 |
| vbc | 0.493000 | 0.454000 | 0.434000 | 0.053000 | 0.034000 | 0.526000 | 0.443000 | 0.524000 | 0.678000 | 0.587000 | 0.542000 | 0.672000 | 0.493000 | 0.452000 | 0.455000 | 0.411000 | 0.411000 | 0.405000 | 0.499000 | 0.510000 | 0.454000 |
| boston | 0.595000 | 0.971000 | 0.837000 | 0.775000 | 0.732000 | 0.783000 | 0.971000 | 0.675000 | 0.581000 | 0.701000 | 0.890000 | 0.682000 | 0.484000 | 0.789000 | 0.954000 | 0.698000 | 0.698000 | 0.588000 | 0.000000 | 0.692000 | 0.790000 |
| AVG | 0.423000 | 0.451000 | 0.410000 | 0.220000 | 0.270000 | 0.521000 | 0.414000 | 0.423000 | 0.434000 | 0.465000 | 0.451000 | 0.454000 | 0.212000 | 0.357000 | 0.388000 | 0.438000 | 0.435000 | 0.379000 | 0.439000 | 0.445000 | 0.300000 |
| WIN | 0.000000 | 2.000000 | 3.000000 | 0.000000 | 0.000000 | 3.000000 | 1.000000 | 2.000000 | 1.000000 | 1.000000 | 1.000000 | 3.000000 | 0.000000 | 0.000000 | 0.000000 | 3.000000 | 4.000000 | 0.000000 | 2.000000 | 1.000000 | 0.000000 |

Fig. 10: Recall performance of 6 CoMadOut (CMO) variants on the left side compared to 14 other anomaly detection algorithms on the right side on 20 real world data sets. The results are based on 100% of all possible principal components.

| dataset | CMO | CMO+ | CMO+k | CMO+e | CMO+ke | CMOEns | PCA-MAD++ | PCA-MAD | HBOS | IF | PCA | PCA(NMI) | LOF | KNN | OC SVM | MCD | EllipticEnv | MLE | AE | VAE | AVG |
|-------------|----------|----------|----------|----------|----------|----------|-----------|----------|----------|----------|----------|----------|----------|----------|----------|----------|-------------|----------|----------|----------|----------|
| arrhythmia | 0.433000 | 0.495000 | 0.503000 | 0.484000 | 0.473000 | 0.472000 | 0.539000 | 0.528000 | 0.443000 | 0.472000 | 0.384000 | 0.399000 | 0.208000 | 0.417000 | 0.343000 | 0.245000 | 0.579000 | 0.280000 | 0.396000 | 0.397000 | 0.424000 |
| cardio | 0.312000 | 0.340000 | 0.377000 | 0.201000 | 0.195000 | 0.383000 | 0.124000 | 0.135000 | 0.441000 | 0.555000 | 0.589000 | 0.268000 | 0.194000 | 0.222000 | 0.329000 | 0.338000 | 0.356000 | 0.462000 | 0.634000 | 0.645000 | 0.355000 |
| anthyroid | 0.493000 | 0.447000 | 0.440000 | 0.437000 | 0.429000 | 0.508000 | 0.575000 | 0.565000 | 0.151000 | 0.256000 | 0.271000 | 0.537000 | 0.081000 | 0.436000 | 0.484000 | 0.504000 | 0.546000 | 0.193000 | 0.207000 | 0.207000 | 0.386000 |
| breastc | 0.964000 | 0.989000 | 0.987000 | 0.984000 | 0.975000 | 0.821000 | 0.905000 | 0.965000 | 0.955000 | 0.963000 | 0.961000 | 0.675000 | 0.274000 | 0.915000 | 0.908000 | 0.871000 | 0.986000 | 0.939000 | 0.768000 | 0.903000 | 0.861000 |
| letter | 0.064000 | 0.059000 | 0.062000 | 0.073000 | 0.082000 | 0.222000 | 0.089000 | 0.069000 | 0.073000 | 0.097000 | 0.072000 | 0.531000 | 0.470000 | 0.301000 | 0.111000 | 0.180000 | 0.180000 | 0.222000 | 0.072000 | 0.075000 | 0.152000 |
| thyroid | 0.815000 | 0.806000 | 0.804000 | 0.801000 | 0.800000 | 0.736000 | 0.788000 | 0.787000 | 0.255000 | 0.521000 | 0.314000 | 0.512000 | 0.047000 | 0.582000 | 0.560000 | 0.700000 | 0.359000 | 0.251000 | 0.444000 | 0.353000 | 0.580000 |
| mammography | 0.021000 | 0.023000 | 0.029000 | 0.028000 | 0.031000 | 0.083000 | 0.016000 | 0.015000 | 0.176000 | 0.168000 | 0.147000 | 0.512000 | 0.113000 | 0.153000 | 0.135000 | 0.038000 | 0.514000 | 0.175000 | 0.195000 | 0.195000 | 0.163000 |
| pinus | 0.468000 | 0.460000 | 0.464000 | 0.457000 | 0.445000 | 0.524000 | 0.433000 | 0.433000 | 0.566000 | 0.491000 | 0.376000 | 0.674000 | 0.415000 | 0.524000 | 0.452000 | 0.486000 | 0.486000 | 0.494000 | 0.393000 | 0.478000 | 0.477000 |
| musk | 0.492000 | 0.667000 | 1.000000 | 0.147000 | 0.042000 | 0.582000 | 0.178000 | 0.225000 | 0.992000 | 0.992000 | 0.998000 | 0.378000 | 0.145000 | 0.081000 | 0.117000 | 1.000000 | 0.612000 | 0.898000 | 1.000000 | 1.000000 | 0.598000 |
| optdigits | 0.025000 | 0.038000 | 0.057000 | 0.063000 | 0.070000 | 0.261000 | 0.027000 | 0.026000 | 0.173000 | 0.061000 | 0.024000 | 0.514000 | 0.028000 | 0.024000 | 0.025000 | 0.024000 | 0.014000 | 0.026000 | 0.026000 | 0.029000 | 0.077000 |
| pendigits | 0.591000 | 0.655000 | 0.603000 | 0.521000 | 0.476000 | 0.452000 | 0.134000 | 0.143000 | 0.239000 | 0.232000 | 0.132000 | 0.511000 | 0.041000 | 0.084000 | 0.204000 | 0.068000 | 0.068000 | 0.055000 | 0.263000 | 0.219000 | 0.285000 |
| mnist | 0.089000 | 0.131000 | 0.142000 | 0.196000 | 0.196000 | 0.437000 | 0.229000 | 0.323000 | 0.067000 | 0.230000 | 0.389000 | 0.548000 | 0.128000 | 0.328000 | 0.106000 | 0.255000 | 0.467000 | 0.380000 | 0.385000 | 0.382000 | 0.270000 |
| shuttle | 0.510000 | 0.233000 | 0.077000 | 0.157000 | 0.077000 | 0.172000 | 0.199000 | 0.183000 | 0.958000 | 0.923000 | 0.112000 | 0.538000 | 0.109000 | 0.245000 | 0.602000 | 0.841000 | 0.365000 | 0.871000 | 0.915000 | 0.915000 | 0.477000 |
| satellite | 0.592000 | 0.601000 | 0.618000 | 0.636000 | 0.649000 | 0.701000 | 0.639000 | 0.644000 | 0.662000 | 0.660000 | 0.654000 | 0.658000 | 0.377000 | 0.536000 | 0.640000 | 0.767000 | 0.767000 | 0.514000 | 0.694000 | 0.696000 | 0.636000 |
| satimage-2 | 0.233000 | 0.925000 | 0.963000 | 0.971000 | 0.973000 | 0.538000 | 0.873000 | 0.964000 | 0.754000 | 0.924000 | 0.885000 | 0.506000 | 0.052000 | 0.336000 | 0.954000 | 0.682000 | 0.682000 | 0.682000 | 0.356000 | 0.889000 | 0.678000 |
| wine | 0.520000 | 0.323000 | 0.472000 | 0.439000 | 0.465000 | 0.566000 | 0.403000 | 0.505000 | 0.365000 | 0.186000 | 0.233000 | 0.535000 | 0.281000 | 0.107000 | 0.198000 | 0.650000 | 0.650000 | 0.103000 | 0.081000 | 0.094000 | 0.359000 |
| vowels | 0.022000 | 0.022000 | 0.022000 | 0.024000 | 0.025000 | 0.210000 | 0.020000 | 0.022000 | 0.074000 | 0.144000 | 0.046000 | 0.517000 | 0.266000 | 0.494000 | 0.119000 | 0.052000 | 0.052000 | 0.347000 | 0.054000 | 0.065000 | 0.130000 |
| glass | 0.076000 | 0.070000 | 0.067000 | 0.073000 | 0.070000 | 0.153000 | 0.058000 | 0.066000 | 0.062000 | 0.084000 | 0.058000 | 0.521000 | 0.111000 | 0.115000 | 0.070000 | 0.080000 | 0.080000 | 0.060000 | 0.051000 | 0.054000 | 0.099000 |
| vbc | 0.485000 | 0.508000 | 0.583000 | 0.366000 | 0.459000 | 0.521000 | 0.552000 | 0.528000 | 0.678000 | 0.587000 | 0.487000 | 0.528000 | 0.493000 | 0.452000 | 0.455000 | 0.411000 | 0.411000 | 0.405000 | 0.482000 | 0.518000 | 0.495000 |
| boston | 0.833000 | 0.812000 | 0.700000 | 0.666000 | 0.585000 | 0.669000 | 0.959000 | 0.959000 | 0.581000 | 0.701000 | 0.836000 | 0.677000 | 0.448000 | 0.789000 | 0.854000 | 0.698000 | 0.679000 | 0.880000 | 0.860000 | 0.857000 | 0.740000 |
| WINE | 0.439000 | 0.425000 | 0.444300 | 0.379000 | 0.390000 | 0.431000 | 0.385000 | 0.399000 | 0.443000 | 0.465000 | 0.435000 | 0.527200 | 0.211200 | 0.357000 | 0.388000 | 0.404000 | 0.435000 | 0.379000 | 0.439000 | 0.437000 | 0.000000 |
| AVG | 1.000000 | 1.000000 | 1.000000 | 0.000000 | 0.000000 | 0.000000 | 2.000000 | 1.000000 | 1.000000 | 1.000000 | 0.000000 | 0.000000 | 0.000000 | 0.000000 | 0.000000 | 3.000000 | 5.000000 | 0.000000 | 1.000000 | 2.000000 | 0.000000 |

| dataset | CMO | CMO+ | CMO+k | CMO+e | CMO+ke | CMOEncs | PCA-MAD++ | PCA-MAD | HBOS | IF | PCA | PCA(NMI) | LOF | KNN | OC SVM | MCD | EllipticEnv | MLE | AE | VAE | AVG |
|-------------|----------|----------|----------|----------|----------|----------|-----------|----------|----------|----------|----------|----------|----------|----------|----------|----------|-------------|----------|----------|----------|----------|
| arrhythmia | 0.466000 | 0.508000 | 0.400000 | 0.292000 | 0.292000 | 0.000000 | 0.503000 | 0.507000 | 0.523000 | 0.462000 | 0.431000 | 0.448000 | 0.231000 | 0.431000 | 0.446000 | 0.323000 | 1.000000 | 0.354000 | 0.431000 | 0.431000 | 0.423000 |
| cardio | 0.489000 | 0.477000 | 0.250000 | 0.080000 | 0.051000 | 0.290000 | 0.579000 | 0.649000 | 0.494000 | 0.484000 | 0.602000 | 0.240000 | 0.222000 | 0.256000 | 0.358000 | 0.483000 | 0.477000 | 0.455000 | 0.645000 | 0.636000 | 0.413000 |
| anethyroid | 0.539000 | 0.560000 | 0.599000 | 0.577000 | 0.573000 | 0.793000 | 0.523000 | 0.481000 | 0.364000 | 0.288000 | 0.238000 | 0.917000 | 0.103000 | 0.455000 | 0.517000 | 0.459000 | 1.000000 | 0.204000 | 0.242000 | 0.242000 | 0.477000 |
| breastc | 0.837000 | 0.846000 | 0.925000 | 0.918000 | 0.775000 | 0.959000 | 0.933000 | 0.933000 | 0.937000 | 0.916000 | 0.929000 | 0.000000 | 0.084000 | 0.908000 | 0.900000 | 0.552000 | 0.937000 | 0.904000 | 0.681000 | 0.816000 | 0.786000 |
| letter | 0.906000 | 0.070000 | 0.100000 | 0.128000 | 0.122000 | 0.000000 | 0.150000 | 0.154000 | 0.060000 | 0.100000 | 0.070000 | 0.000000 | 0.420000 | 0.330000 | 0.160000 | 0.170000 | 0.170000 | 0.280000 | 0.070000 | 0.070000 | 0.135000 |
| thyroid | 0.731000 | 0.720000 | 0.731000 | 0.710000 | 0.710000 | 0.000000 | 0.640000 | 0.599000 | 0.312000 | 0.527000 | 0.355000 | 0.672000 | 0.065000 | 0.599000 | 0.591000 | 0.656000 | 1.000000 | 0.280000 | 0.430000 | 0.366000 | 0.544000 |
| mammography | 0.051000 | 0.046000 | 0.162000 | 0.042000 | 0.052000 | 0.290000 | 0.333000 | 0.295000 | 0.152000 | 0.165000 | 0.258000 | 0.000000 | 0.000000 | 0.227000 | 0.219000 | 0.058000 | 1.000000 | 0.269000 | 0.238000 | 0.258000 | 0.200000 |
| pima | 0.521000 | 0.539000 | 0.517000 | 0.468000 | 0.423000 | 0.518000 | 0.556000 | 0.558000 | 0.543000 | 0.513000 | 0.468000 | 0.000000 | 0.431000 | 0.539000 | 0.468000 | 0.513000 | 0.513000 | 0.506000 | 0.446000 | 0.401000 | 0.475000 |
| musk | 0.188000 | 0.188000 | 0.188000 | 0.000000 | 0.000000 | 0.000000 | 1.000000 | 1.000000 | 0.979000 | 0.926000 | 0.990000 | 0.188000 | 0.219000 | 0.104000 | 0.125000 | 1.000000 | 1.000000 | 0.812000 | 1.000000 | 0.990000 | 0.545000 |
| optdigits | 0.000000 | 0.007000 | 0.000000 | 0.009000 | 0.009000 | 0.000000 | 0.001000 | 0.000000 | 0.333000 | 0.040000 | 0.000000 | 0.000000 | 0.033000 | 0.007000 | 0.000000 | 0.000000 | 0.000000 | 0.000000 | 0.000000 | 0.000000 | 0.025000 |
| pendigits | 0.314000 | 0.301000 | 0.186000 | 0.013000 | 0.013000 | 0.000000 | 0.271000 | 0.283000 | 0.301000 | 0.295000 | 0.327000 | 0.000000 | 0.077000 | 0.128000 | 0.314000 | 0.103000 | 0.103000 | 0.045000 | 0.327000 | 0.333000 | 0.187000 |
| mnist | 0.067000 | 0.347000 | 0.389000 | 0.287000 | 0.289000 | 0.000000 | 0.535000 | 0.562000 | 0.033000 | 0.243000 | 0.384000 | 0.167000 | 0.141000 | 0.366000 | 0.064000 | 0.279000 | 0.833000 | 0.396000 | 0.390000 | 0.417000 | 0.310000 |
| shuttle | 0.623000 | 0.635000 | 0.178000 | 0.913000 | 0.181000 | 0.000000 | 0.961000 | 0.955000 | 0.913000 | 0.940000 | 0.951000 | 0.546000 | 0.138000 | 0.289000 | 0.627000 | 0.744000 | 0.000000 | 0.858000 | 0.946000 | 0.951000 | 0.628000 |
| satellite | 0.496000 | 0.541000 | 0.536000 | 0.618000 | 0.524000 | 0.854000 | 0.641000 | 0.640000 | 0.574000 | 0.569000 | 0.484000 | 0.000000 | 0.369000 | 0.950000 | 0.901000 | 0.654000 | 0.685000 | 0.456000 | 0.564000 | 0.980000 | 0.532000 |
| satimage-2 | 0.901000 | 0.901000 | 0.930000 | 0.223000 | 0.211000 | 0.000000 | 0.929000 | 0.932000 | 0.690000 | 0.859000 | 0.831000 | 0.000000 | 0.070000 | 0.394000 | 0.901000 | 0.634000 | 0.634000 | 0.366000 | 0.831000 | 0.831000 | 0.604000 |
| wine | 0.333000 | 0.222000 | 0.333000 | 0.000000 | 0.000000 | 0.000000 | 0.410000 | 0.480000 | 0.442000 | 0.111000 | 0.222000 | 0.000000 | 0.333000 | 0.000000 | 0.222000 | 0.444000 | 0.444000 | 0.000000 | 0.111000 | 0.111000 | 0.211000 |
| vowels | 0.080000 | 0.120000 | 0.030000 | 0.040000 | 0.040000 | 0.000000 | 0.241000 | 0.241000 | 0.120000 | 0.220000 | 0.140000 | 0.000000 | 0.340000 | 0.500000 | 0.220000 | 0.060000 | 0.060000 | 0.380000 | 0.140000 | 0.140000 | 0.169000 |
| glass | 0.000000 | 0.000000 | 0.000000 | 0.111000 | 0.111000 | 0.000000 | 0.5123000 | 0.123000 | 0.000000 | 0.111000 | 0.111000 | 0.000000 | 0.111000 | 0.111000 | 0.111000 | 0.000000 | 0.000000 | 0.111000 | 0.111000 | 0.111000 | 0.062000 |
| vbc | 0.571000 | 0.524000 | 0.524000 | 0.095000 | 0.046000 | 0.000000 | 0.562000 | 0.551000 | 0.619000 | 0.619000 | 0.571000 | 0.571000 | 0.524000 | 0.524000 | 0.524000 | 0.429000 | 0.429000 | 0.429000 | 0.476000 | 0.476000 | 0.453000 |
| boston | 0.877000 | 0.894000 | 0.689000 | 0.654000 | 0.564000 | 1.000000 | 0.894000 | 0.927000 | 0.475000 | 0.665000 | 0.786000 | 1.000000 | 0.469000 | 0.715000 | 0.877000 | 0.592000 | 1.000000 | 0.598000 | 0.754000 | 0.793000 | 0.762000 |
| avg | 0.407000 | 0.427000 | 0.397000 | 0.308000 | 0.248000 | 0.220000 | 0.539000 | 0.542000 | 0.432000 | 0.453000 | 0.459000 | 0.247000 | 0.229000 | 0.367000 | 0.409000 | 0.409000 | 0.564000 | 0.385000 | 0.442000 | 0.444000 | 0.000000 |
| WHN | 0.000000 | 0.000000 | 0.000000 | 0.000000 | 0.000000 | 3.000000 | 2.000000 | 6.000000 | 2.000000 | 1.000000 | 0.000000 | 1.000000 | 1.000000 | 1.000000 | 0.000000 | 1.000000 | 7.000000 | 0.000000 | 2.000000 | 1.000000 | 0.000000 |

Fig. 12: Precision@n (P@n) performance of 6 CoMadOut (CMO) variants on the left side compared to 14 other anomaly detection algorithms on the right side on 20 real world data sets. The results are based on 100% of all possible principal components.

| dataset | CMO | CMO+ | CMO+k | CMO+e | CMO+ke | CMOEncs | PCA-MAD++ | PCA-MAD | HBOS | IF | PCA | PCA(NMI) | LOF | KNN | OC SVM | MCD | EllipticEnv | MLE | AE | VAE | AVG |
|-------------|----------|----------|----------|----------|----------|----------|-----------|----------|----------|----------|----------|----------|----------|----------|----------|----------|-------------|----------|----------|----------|----------|
| arrhythmia | 0.462000 | 0.477000 | 0.492000 | 0.446000 | 0.415000 | 0.562000 | 0.503000 | 0.507000 | 0.523000 | 0.462000 | 0.431000 | 0.415000 | 0.231000 | 0.431000 | 0.446000 | 0.338000 | 1.000000 | 0.354000 | 0.431000 | 0.431000 | 0.468000 |
| cardio | 0.301000 | 0.364000 | 0.392000 | 0.239000 | 0.222000 | 0.000000 | 0.579000 | 0.649000 | 0.494000 | 0.484000 | 0.591000 | 0.429000 | 0.222000 | 0.256000 | 0.358000 | 0.455000 | 0.477000 | 0.455000 | 0.642000 | 0.648000 | 0.413000 |
| anethyroid | 0.545000 | 0.418000 | 0.419000 | 0.412000 | 0.406000 | 0.680000 | 0.520000 | 0.451000 | 0.364000 | 0.288000 | 0.305000 | 0.000000 | 0.103000 | 0.455000 | 0.517000 | 0.459000 | 1.000000 | 0.204000 | 0.242000 | 0.251000 | 0.397000 |
| breastc | 0.744000 | 0.904000 | 0.877000 | 0.777000 | 0.709000 | 0.925000 | 0.933000 | 0.933000 | 0.937000 | 0.916000 | 0.952000 | 0.000000 | 0.084000 | 0.908000 | 0.900000 | 0.552000 | 0.937000 | 0.904000 | 0.661000 | 0.661000 | 0.7430 |
| letter | 0.060000 | 0.040000 | 0.060000 | 0.080000 | 0.100000 | 0.000000 | 0.150000 | 0.154000 | 0.060000 | 0.100000 | 0.080000 | 0.000000 | 0.420000 | 0.330000 | 0.160000 | 0.170000 | 0.170000 | 0.280000 | 0.080000 | 0.080000 | 0.127000 |
| thyroid | 0.774000 | 0.742000 | 0.731000 | 0.731000 | 0.731000 | 0.744000 | 0.640000 | 0.599000 | 0.312000 | 0.527000 | 0.372000 | 0.000000 | 0.065000 | 0.599000 | 0.591000 | 0.656000 | 1.000000 | 0.280000 | 0.462000 | 0.344000 | 0.551000 |
| mammography | 0.008000 | 0.023000 | 0.035000 | 0.050000 | 0.027000 | 0.000000 | 0.333000 | 0.295000 | 0.152000 | 0.165000 | 0.238000 | 0.000000 | 0.227000 | 0.227000 | 0.219000 | 0.065000 | 1.000000 | 0.269000 | 0.258000 | 0.208000 | 0.190000 |
| pima | 0.461000 | 0.487000 | 0.476000 | 0.487000 | 0.483000 | 0.468000 | 0.556000 | 0.558000 | 0.543000 | 0.513000 | 0.378000 | 0.000000 | 0.431000 | 0.539000 | 0.468000 | 0.513000 | 0.513000 | 0.506000 | 0.404000 | 0.506000 | 0.465000 |
| musk | 0.510000 | 0.719000 | 1.000000 | 0.042000 | 0.050000 | 0.000000 | 1.000000 | 1.000000 | 0.979000 | 0.926000 | 0.969000 | 0.474000 | 0.219000 | 0.104000 | 0.125000 | 1.000000 | 1.000000 | 0.812000 | 0.990000 | 0.990000 | 0.668000 |
| optdigits | 0.013000 | 0.000000 | 0.000000 | 0.000000 | 0.000000 | 0.000000 | 0.001000 | 0.000000 | 0.333000 | 0.040000 | 0.000000 | 0.000000 | 0.033000 | 0.007000 | 0.000000 | 0.000000 | 0.000000 | 0.000000 | 0.000000 | 0.000000 | 0.016000 |
| pendigits | 0.351000 | 0.609000 | 0.564000 | 0.519000 | 0.494000 | 0.000000 | 0.271000 | 0.283000 | 0.301000 | 0.295000 | 0.250000 | 0.000000 | 0.077000 | 0.128000 | 0.314000 | 0.103000 | 0.103000 | 0.045000 | 0.365000 | 0.340000 | 0.281000 |
| mnist | 0.033000 | 0.163000 | 0.166000 | 0.267000 | 0.271000 | 0.000000 | 0.535000 | 0.562000 | 0.033000 | 0.243000 | 0.386000 | 0.000000 | 0.141000 | 0.366000 | 0.064000 | 0.234000 | 0.833000 | 0.396000 | 0.389000 | 0.386000 | 0.273000 |
| shuttle | 0.515000 | 0.304000 | 0.079000 | 0.173000 | 0.079000 | 0.264000 | 0.961000 | 0.965000 | 0.913000 | 0.940000 | 0.950000 | 0.000000 | 0.138000 | 0.289000 | 0.627000 | 0.744000 | 0.000000 | 0.858000 | 0.951000 | 0.951000 | 0.535000 |
| satellite | 0.456000 | 0.485000 | 0.466000 | 0.533000 | 0.543000 | 0.808000 | 0.641000 | 0.640000 | 0.574000 | 0.569000 | 0.534000 | 0.000000 | 0.369000 | 0.495000 | 0.516000 | 0.685000 | 0.685000 | 0.456000 | 0.560000 | 0.563000 | 0.530000 |
| satimage-2 | 0.254000 | 0.888000 | 0.901000 | 0.930000 | 0.930000 | 0.000000 | 0.929000 | 0.932000 | 0.690000 | 0.859000 | 0.803000 | 0.000000 | 0.070000 | 0.394000 | 0.901000 | 0.634000 | 0.634000 | 0.366000 | 0.831000 | 0.831000 | 0.639000 |
| wine | 0.444000 | 0.333000 | 0.556000 | 0.556000 | 0.556000 | 0.000000 | 0.410000 | 0.480000 | 0.444000 | 0.111000 | 0.111000 | 0.000000 | 0.333000 | 0.000000 | 0.222000 | 0.444000 | 0.444000 | 0.000000 | 0.111000 | 0.111000 | 0.283000 |
| vowels | 0.000000 | 0.000000 | 0.020000 | 0.020000 | 0.020000 | 0.000000 | 0.241000 | 0.241000 | 0.120000 | 0.220000 | 0.080000 | 0.000000 | 0.340000 | 0.500000 | 0.220000 | 0.060000 | 0.060000 | 0.380000 | 0.140000 | 0.140000 | 0.140000 |
| glass | 0.000000 | 0.000000 | 0.000000 | 0.000000 | 0.000000 | 0.000000 | 0.123000 | 0.123000 | 0.000000 | 0.111000 | 0.111000 | 0.000000 | 0.111000 | 0.111000 | 0.111000 | 0.000000 | 0.000000 | 0.111000 | 0.111000 | 0.111000 | 0.057000 |
| vbc | 0.381000 | 0.476000 | 0.571000 | 0.476000 | 0.476000 | 0.000000 | 0.562000 | 0.551000 | 0.619000 | 0.619000 | 0.476000 | 0.000000 | 0.524000 | 0.524000 | 0.524000 | 0.429000 | 0.429000 | 0.429000 | 0.476000 | 0.524000 | 0.453000 |
| boston | 0.737000 | 0.726000 | 0.626000 | 0.690000 | 0.536000 | 0.688000 | 0.965000 | 0.961000 | 0.475000 | 0.665000 | 0.721000 | 0.000000 | 0.469000 | 0.715000 | 0.877000 | 0.932000 | 1.000000 | 0.598000 | 0.754000 | 0.754000 | 0.668000 |
| WIG | 0.036000 | 0.408000 | 0.421000 | 0.367000 | 0.375000 | 0.257000 | 0.540000 | 0.541000 | 0.433000 | 0.433000 | 0.426000 | 0.066000 | 0.229000 | 0.367000 | 0.400000 | 0.407000 | 0.564000 | 0.385000 | 0.442000 | 0.441000 | 0.000000 |
| AVN | 0.000000 | 0.000000 | 0.000000 | 0.000000 | 0.000000 | 0.000000 | 2.000000 | 0.000000 | 3.000000 | 1.000000 | 0.000000 | 0.000000 | 0.000000 | 0.000000 | 0.000000 | 0.000000 | 0.000000 | 0.000000 | 0.000000 | 0.000000 | 0.000000 |

| dataset | CMO | CMO+ | CMO-k | CMO-e | CMO-ke | CMOEm | PCA-MAD++ | PCA-MAD | HBOS | IF | PCA | PCAINMI | LOF | KNN | OC5VM | MCD | EllipticEnv | MLE | AE | VAE | AVG |
|-------------|-----------|-----------|-----------|-----------|-----------|-----------|-----------|----------|-----------|----------|----------|-----------|-----------|-----------|-----------|-----------|-------------|-----------|------------|------------|-----------|
| anthyemia | 45.637000 | 46.401000 | 46.401000 | 46.401000 | 46.401000 | 46.401000 | 0.317700 | 0.255000 | 2.142000 | 0.446000 | 0.120000 | 12.798000 | 0.137000 | 0.222000 | 0.114000 | 3.591000 | 0.182000 | 12.859000 | 9.876000 | 16.281000 | |
| cardio | 0.978000 | 0.732000 | 0.732000 | 0.732000 | 0.732000 | 0.732000 | 0.034000 | 0.038000 | 0.009000 | 0.443000 | 0.017000 | 0.620000 | 0.178000 | 0.303000 | 0.326000 | 0.949000 | 1.007000 | 0.021000 | 26.898000 | 29.555000 | 3.231000 |
| anthyroid | 0.697000 | 0.421000 | 0.421000 | 0.421000 | 0.421000 | 0.421000 | 0.013000 | 0.011000 | 0.005000 | 0.725000 | 0.007000 | 0.467000 | 1.371000 | 1.832000 | 4.168000 | 2.296000 | 2.426000 | 0.223000 | 95.192000 | 109.271000 | 1.046000 |
| breastse | 0.131000 | 0.107000 | 0.107000 | 0.107000 | 0.107000 | 0.107000 | 0.008000 | 0.009000 | 0.003000 | 0.345000 | 0.001000 | 0.076000 | 0.091000 | 0.105000 | 0.048000 | 0.658000 | 0.701000 | 0.011000 | 12.619000 | 12.619000 | 1.389000 |
| letter | 1.572000 | 1.315000 | 1.315000 | 1.315000 | 1.315000 | 1.315000 | 0.060000 | 0.085000 | 0.013000 | 0.447000 | 0.009000 | 0.973000 | 0.220000 | 0.338000 | 0.254000 | 4.549000 | 4.669000 | 0.013000 | 23.234000 | 26.658000 | 3.484000 |
| thyroid | 0.407000 | 0.266000 | 0.266000 | 0.266000 | 0.266000 | 0.266000 | 0.011000 | 0.011000 | 0.004000 | 0.532000 | 0.004000 | 0.270000 | 0.344000 | 0.662000 | 1.433000 | 1.485000 | 1.483000 | 0.062000 | 51.465000 | 59.787000 | 5.964000 |
| mammography | 1.455000 | 1.186000 | 1.186000 | 1.186000 | 1.186000 | 1.186000 | 0.023000 | 0.016000 | 0.007000 | 1.080000 | 0.017000 | 0.899000 | 1.474000 | 2.219000 | 10.566000 | 2.573000 | 2.118000 | 0.502000 | 151.121000 | 170.965000 | 17.549000 |
| pima | 0.145000 | 0.101000 | 0.101000 | 0.101000 | 0.101000 | 0.101000 | 0.010000 | 0.008000 | 0.004000 | 0.412000 | 0.004000 | 0.132000 | 0.302000 | 0.088000 | 0.047000 | 0.739000 | 0.684000 | 0.003000 | 12.546000 | 14.655000 | 1.500000 |
| musk | 46.793000 | 44.808000 | 44.808000 | 44.808000 | 44.808000 | 44.808000 | 0.254000 | 0.317000 | 0.002000 | 1.352000 | 0.207000 | 32.560000 | 3.354000 | 4.112000 | 2.383000 | 9.064000 | 6.014000 | 0.398000 | 43.019000 | 50.876000 | 26.10000 |
| optdigits | 0.173000 | 0.1468000 | 0.1468000 | 0.1468000 | 0.1468000 | 0.1468000 | 0.127000 | 0.137000 | 0.044000 | 1.195000 | 0.086000 | 11.681000 | 3.875000 | 4.099000 | 3.042000 | 10.768000 | 6.986000 | 0.151000 | 12.317000 | 12.619000 | 13.423000 |
| pendigits | 1.985000 | 1.361000 | 1.361000 | 1.361000 | 1.361000 | 1.361000 | 0.048000 | 0.029000 | 0.015000 | 0.877000 | 0.013000 | 1.578000 | 1.826000 | 2.153000 | 4.333000 | 8.450000 | 6.375000 | 0.215000 | 144.681000 | 154.765000 | 14.268000 |
| mnist | 37.919000 | 34.561000 | 34.561000 | 34.561000 | 34.561000 | 34.561000 | 0.299000 | 0.326000 | 0.077000 | 2.247000 | 0.195000 | 34.089000 | 15.131000 | 16.328000 | 17.631000 | 18.265000 | 17.516000 | 0.417000 | 106.199000 | 120.977000 | 27.963000 |
| shuttle | 7.793000 | 4.253000 | 4.253000 | 4.253000 | 4.253000 | 4.253000 | 0.067000 | 0.098000 | 0.010000 | 4.900000 | 0.039000 | 5.309000 | 5.124800 | 5.747000 | 23.079000 | 65.467000 | 30.429000 | 32.612000 | 655.250000 | 750.592000 | 95.969000 |
| satellite | 6.573000 | 4.693000 | 4.693000 | 4.693000 | 4.693000 | 4.693000 | 0.094000 | 0.077000 | 0.024000 | 0.966000 | 0.041000 | 4.955000 | 2.356000 | 2.644000 | 4.473000 | 10.070000 | 13.574000 | 0.195000 | 144.440000 | 105.771000 | 16.955000 |
| satimage-2 | 5.536000 | 4.719000 | 4.719000 | 4.719000 | 4.719000 | 4.719000 | 0.077000 | 0.100000 | 0.023000 | 1.021000 | 0.047000 | 4.898000 | 1.558000 | 2.151000 | 3.891000 | 16.651000 | 10.198000 | 0.174000 | 79.940000 | 89.494000 | 12.31000 |
| vine | 0.171000 | 0.141000 | 0.141000 | 0.141000 | 0.141000 | 0.141000 | 0.010000 | 0.005000 | 0.003000 | 0.337000 | 0.004000 | 0.065000 | 0.095000 | 0.030000 | 0.030000 | 0.050000 | 0.057000 | 0.002000 | 3.960000 | 4.299000 | 0.550000 |
| vowels | 0.342000 | 0.236000 | 0.236000 | 0.236000 | 0.236000 | 0.236000 | 0.012000 | 0.012000 | 0.005000 | 0.406000 | 0.004000 | 0.246000 | 0.060000 | 0.189000 | 0.173000 | 1.164000 | 1.274000 | 0.008000 | 23.165000 | 24.944000 | 2.660000 |
| glass | 0.083000 | 0.065000 | 0.065000 | 0.065000 | 0.065000 | 0.065000 | 0.009000 | 0.009000 | 0.004000 | 0.309000 | 0.003000 | 0.632000 | 0.050000 | 0.020000 | 0.050000 | 0.045000 | 0.045000 | 0.002000 | 3.343000 | 5.890000 | 0.609000 |
| wbc | 0.736000 | 0.649000 | 0.649000 | 0.649000 | 0.649000 | 0.649000 | 0.035000 | 0.025000 | 0.011000 | 0.334000 | 0.055000 | 0.307000 | 0.010000 | 0.043000 | 0.017000 | 0.172000 | 0.142000 | 0.004000 | 7.510000 | 8.127000 | 1.036000 |
| boston | 0.210000 | 0.178000 | 0.178000 | 0.178000 | 0.178000 | 0.178000 | 0.010000 | 0.012000 | 0.005000 | 0.316000 | 0.003000 | 0.098000 | 0.010000 | 0.052000 | 0.026000 | 0.899000 | 0.878000 | 0.016000 | 10.194000 | 10.707000 | 1.216000 |
| AVG | 8.653000 | 7.895000 | 7.895000 | 7.895000 | 7.895000 | 7.895000 | 0.079000 | 0.071000 | 0.017000 | 0.126000 | 0.014000 | 0.941000 | 5.623000 | 4.188000 | 4.546000 | 14.311000 | 16.299000 | 0.317000 | 126.90000 | 84.097000 | 9.859000 |
| WIN | 0.000000 | 0.000000 | 0.000000 | 0.000000 | 0.000000 | 0.000000 | 0.000000 | 0.000000 | 11.000000 | 0.000000 | 6.000000 | 0.000000 | 0.000000 | 0.000000 | 1.000000 | 0.000000 | 0.000000 | 4.000000 | 0.000000 | 0.000000 | 0.000000 |

Fig. 14: Runtime in seconds of 6 CoMadOut (CMO) variants on the left side compared to 14 other anomaly detection algorithms on the right side on 20 real world data sets. The results are based on 100% of all possible principal components.

| dataset | CMO | CMO+ | CMO-k | CMO-e | CMO-ke | CMOEm | PCA-MAD++ | PCA-MAD | HBOS | IF | PCA | PCAINMI | LOF | KNN | OC5VM | MCD | EllipticEnv | MLE | AE | VAE | AVG |
|-------------|-----------|-----------|-----------|-----------|-----------|-----------|-----------|----------|----------|----------|----------|----------|-----------|-----------|------------|-----------|-------------|-----------|------------|------------|-----------|
| anthyemia | 34.122000 | 34.173000 | 34.173000 | 34.173000 | 34.173000 | 34.173000 | 0.150000 | 0.231000 | 2.197000 | 0.458000 | 0.042000 | 1.147000 | 0.139000 | 0.178000 | 0.083000 | 2.821000 | 4.535000 | 0.166000 | 12.789000 | 9.885000 | 11.995000 |
| cardio | 0.407000 | 0.310000 | 0.310000 | 0.310000 | 0.310000 | 0.310000 | 0.059000 | 0.052000 | 0.003000 | 0.441000 | 0.010000 | 0.251000 | 0.176000 | 0.307000 | 0.331000 | 0.264000 | 1.938000 | 0.031000 | 27.126000 | 30.818000 | 3.278000 |
| anthyroid | 0.300000 | 0.176000 | 0.176000 | 0.176000 | 0.176000 | 0.176000 | 0.045000 | 0.035000 | 0.005000 | 0.745000 | 0.005000 | 0.214000 | 1.353000 | 1.895000 | 4.155000 | 2.344000 | 2.197000 | 0.203000 | 96.693000 | 110.951000 | 11.101000 |
| breastse | 0.106000 | 0.064000 | 0.064000 | 0.064000 | 0.064000 | 0.064000 | 0.007000 | 0.006000 | 0.004000 | 0.346000 | 0.003000 | 0.031000 | 0.019000 | 0.067000 | 0.039000 | 0.757000 | 0.851000 | 0.006000 | 11.486000 | 13.530000 | 1.379000 |
| letter | 0.168000 | 0.700000 | 0.700000 | 0.700000 | 0.700000 | 0.700000 | 0.061000 | 0.055000 | 0.014000 | 0.447000 | 0.015000 | 0.254000 | 0.211000 | 0.360000 | 0.256000 | 3.970000 | 41.203000 | 0.019000 | 22.994000 | 26.593000 | 5.036000 |
| thyroid | 0.239000 | 0.105000 | 0.105000 | 0.105000 | 0.105000 | 0.105000 | 0.043000 | 0.036000 | 0.004000 | 0.558000 | 0.004000 | 0.120000 | 0.388000 | 0.639000 | 1.061000 | 1.522000 | 1.500000 | 0.061000 | 52.348000 | 84.548000 | 7.175000 |
| mammography | 0.425000 | 0.262000 | 0.262000 | 0.262000 | 0.262000 | 0.262000 | 0.035000 | 0.020000 | 0.007000 | 0.999000 | 0.006000 | 0.243000 | 1.439000 | 2.240000 | 10.265000 | 2.562000 | 2.123000 | 0.516000 | 151.621000 | 173.458000 | 17.463000 |
| pima | 0.088000 | 0.053000 | 0.053000 | 0.053000 | 0.053000 | 0.053000 | 0.010000 | 0.006000 | 0.003000 | 0.346000 | 0.003000 | 0.029000 | 0.025000 | 0.117000 | 0.049000 | 0.729000 | 0.772000 | 0.003000 | 11.808000 | 13.338000 | 1.378000 |
| musk | 16.693000 | 16.011000 | 16.011000 | 16.011000 | 16.011000 | 16.011000 | 0.810000 | 0.712000 | 0.074000 | 1.199000 | 0.081000 | 3.026000 | 3.917000 | 3.594000 | 2.482000 | 52.969000 | 54.071000 | 0.314000 | 41.107000 | 47.371000 | 15.177000 |
| optdigits | 3.355000 | 3.122000 | 3.122000 | 3.122000 | 3.122000 | 3.122000 | 0.107000 | 0.089000 | 0.041000 | 1.021000 | 0.038000 | 1.302000 | 3.768000 | 4.185000 | 3.414000 | 5.719000 | 9.649000 | 0.205000 | 73.717000 | 83.886000 | 10.319000 |
| pendigits | 0.747000 | 0.459000 | 0.459000 | 0.459000 | 0.459000 | 0.459000 | 0.063000 | 0.057000 | 0.014000 | 0.891000 | 0.012000 | 0.525000 | 1.882000 | 2.274000 | 4.302000 | 7.395000 | 6.530000 | 0.211000 | 95.166000 | 108.457000 | 11.546000 |
| mnist | 11.248000 | 8.067000 | 8.067000 | 8.067000 | 8.067000 | 8.067000 | 0.277000 | 0.230000 | 0.074000 | 2.268000 | 0.075000 | 3.668000 | 14.861000 | 18.473000 | 18.336000 | 14.175000 | 14.345000 | 0.512000 | 104.964000 | 120.614000 | 18.217000 |
| shuttle | 2.379000 | 1.534000 | 1.534000 | 1.534000 | 1.534000 | 1.534000 | 0.175000 | 0.207000 | 0.038000 | 4.546000 | 0.031000 | 2.323000 | 55.873000 | 55.979000 | 232.157000 | 82.133000 | 34.967000 | 50.491000 | 676.273000 | 747.609000 | 97.642000 |
| satellite | 1.893000 | 1.404000 | 1.404000 | 1.404000 | 1.404000 | 1.404000 | 0.115000 | 0.103000 | 0.025000 | 0.626000 | 0.020000 | 0.940000 | 2.371000 | 2.642000 | 4.769000 | 31.647000 | 24.639000 | 0.254000 | 86.683000 | 99.973000 | 13.203000 |
| satimage-2 | 1.760000 | 1.229000 | 1.229000 | 1.229000 | 1.229000 | 1.229000 | 0.073000 | 0.102000 | 0.022000 | 0.961000 | 0.019000 | 0.801000 | 1.933000 | 2.349000 | 3.785000 | 11.006000 | 10.259000 | 0.181000 | 80.223000 | 92.524000 | 10.603000 |
| vine | 0.093000 | 0.097000 | 0.097000 | 0.097000 | 0.097000 | 0.097000 | 0.007000 | 0.009000 | 0.007000 | 0.331000 | 0.003000 | 0.013000 | 0.004000 | 0.014000 | 0.004000 | 0.067000 | 0.064000 | 0.002000 | 4.154000 | 4.740000 | 0.500000 |
| vowels | 0.194000 | 0.130000 | 0.130000 | 0.130000 | 0.130000 | 0.130000 | 0.010000 | 0.009000 | 0.008000 | 0.407000 | 0.003000 | 0.074000 | 0.004000 | 0.019000 | 0.176000 | 1.250000 | 1.169000 | 0.009000 | 21.601000 | 24.134000 | 2.499000 |
| glass | 0.051000 | 0.049000 | 0.049000 | 0.049000 | 0.049000 | 0.049000 | 0.005000 | 0.005000 | 0.004000 | 0.300000 | 0.003000 | 0.012000 | 0.005000 | 0.019000 | 0.005000 | 0.049000 | 0.056000 | 0.003000 | 4.950000 | 7.011000 | 0.636000 |
| wbc | 0.620000 | 0.444000 | 0.444000 | 0.444000 | 0.444000 | 0.444000 | 0.016000 | 0.014000 | 0.011000 | 0.348000 | 0.004000 | 0.048000 | 0.016000 | 0.061000 | 0.019000 | 1.822000 | 4.399000 | 0.004000 | 7.948000 | 8.648000 | 1.308000 |
| insect | 0.159000 | 0.121000 | 0.121000 | 0.121000 | 0.121000 | 0.121000 | 0.012000 | 0.010000 | 0.005000 | 0.328000 | 0.003000 | 0.040000 | 0.017000 | 0.026000 | 0.025000 | 0.927000 | 0.920000 | 0.003000 | 9.156000 | 10.318000 | 1.000000 |
| AVG | 3.781000 | 3.425000 | 3.425000 | 3.425000 | 3.425000 | 3.425000 | 0.094000 | 0.074000 | 0.128000 | 0.689000 | 0.009000 | 0.750000 | 4.938000 | 4.782000 | 14.268000 | 11.262000 | 10.609000 | 2.660000 | 79.737000 | 90.902000 | 0.000000 |
| Win | 0.000000 | 0.000000 | 0.000000 | 0.000000 | 0.000000 | 0.000000 | 0.000000 | 0.000000 | 0.000000 | 0.000000 | 0.000000 | 0.000000 | 0.000000 | 0.000000 | 0.000000 | 0.000000 | 0.000000 | 0.000000 | 0.000000 | 0.000000 | 0.000000 |

than PCA and on heavily reduced number of principal components even the best recall performance among all compared methods.

The evidence for the contribution of the coMAD-based outlier scoring is shown by the CoMadOut variant CMO+ which shows on par with the kurtosis-weighted variant CMO+k an competitive average performance to the majority of all other outlier detection algorithms in terms of AP and AUROC. The evidence for the contribution of the distribution tailedness based outlier score weighting is shown when comparing related CoMadOut variant CMO+k with the most related variance- and z-score-weighted approaches of PCA-MAD. In terms of average precision CMO+k outperforms the related PCA-MAD approaches and shows a competitive overall performance also in terms of recall on a reduced number of principal components.

The evidence for robustness is especially shown when comparing CoMadOut with outlier-robust methods like PCA-MAD, MCD, etc. and outlier-sensitive methods like PCA, MLE, etc. on data sets with a high percentage of outliers and noise. On the majority of these data sets CoMadOut shows compared to the outlier-sensitive methods and partially even also to robust outlier detection methods a better performance in terms of AP, AUROC and recall. Furthermore, the difference is directly visible when comparing the test data set plots of the principal components of coMAD-PCA and standard PCA next to each other where those of standard PCA are sensitive towards the shown outlier (cf. Fig. 2).

5 Conclusion

In this work we proposed CoMadOut, a robust outlier detection algorithm using coMAD-PCA in order to apply PCA without sensitivity to outliers providing an initially selective inlier region besides an extending inlier noise margin by measures of in-distribution (ID) and measures of out-of-distribution (OOD). They care for distribution based alignment of the outlier scores of each principal component, and with that, for an appropriate alignment of the decision boundary between normal and abnormal instances. Based on the assumption that samples are only considered as outliers when they are not part of our enhanced inlier region or when they exceed the distribution tailedness weighted outlier score boundary, we demonstrated an on par performance to various kinds of (robust) state-of-the-art outlier detection methods. The consideration of estimating the ideal number of principal components, spatial outlier constraints as well as the parallelization of CoMadOut in a future work could make our approach efficiently applicable to high-dimensional data sets and thereby also beneficial to other application domains with the requirement of robust outlier detection.

Declarations

- Funding - This work has been funded by the German Federal Ministry of Education and Research (BMBF) under Grant No. 01IS18036A. The authors of this work take full responsibility for its content.
- Conceptualization: Andreas Lohrer (Lead), Daniyal Kazempour (Supporting), Peer Kröger (Supporting)
- Methodology: Andreas Lohrer (Lead), Daniyal Kazempour (Supporting)
- Formal Analysis: Andreas Lohrer (Lead)
- Writing – original draft: Andreas Lohrer (Lead), Daniyal Kazempour (Supporting), Max Hünemörder (Supporting), Peer Kröger (Supporting)
- Writing – review & editing: Andreas Lohrer (Lead), Daniyal Kazempour (Supporting), Peer Kröger (Supporting)
- Implementation: Andreas Lohrer (Lead)
- Funding acquisition - Peer Kröger (Lead)
- Employment, Financial interests, Non-Financial interests - Not applicable
- Conflict of interest/Competing interests - No conflicts to declare.
- Ethics approval - Not applicable
- Consent to participate/publication - Not applicable (all agree)
- Employment, Financial interests, Non-Financial interests - Not applicable
- Availability of data and materials - Not applicable (publicly available)
- Code availability - Will be publicly available at <https://github.com/lohrera/CoMadOut>

The idea for the approach and article had Andreas Lohrer. The literature research had been conducted by Max Hünemörder, Andreas Lohrer and Daniyal Kazempour. The article had been written by Andreas Lohrer, Daniyal Kazempour, Maximilian Hünemörder, and Peer Kröger. The introduced approach has been implemented and evaluated by Andreas Lohrer. All authors critically revised the work.

References

- Aggarwal, C.C. (2016). *Outlier analysis* (2nd ed.). New York: Springer.
- An, J., & Cho, S. (2015). Variational autoencoder based anomaly detection using reconstruction probability. *Special Lecture on IE*, 2(1), 1–18.
- Breunig, M.M., Kriegel, H.-P., Ng, R.T., Sander, J. (2000). LOF: Identifying Density-Based Local Outliers. *Proceedings of the 2000 ACM SIGMOD International Conference on Management of Data* (p. 93–104). New York, NY, USA: Association for Computing Machinery.
- Campos, G.O., Zimek, A., Sander, J., Campello, R.J., Micenková, B., Schubert, E., ... Houle, M.E. (2016, jul). On the Evaluation of Unsupervised Outlier Detection: Measures, Datasets, and an Empirical Study. *Data Min. Knowl. Discov.*, 30(4), 891–927.

- Candès, E.J., Li, X., Ma, Y., Wright, J. (2011). Robust principal component analysis? *J. ACM*, 58(3), 11.
- Crammer, K., & Chechik, G. (2004). A Needle in a Haystack: Local One-Class Optimization. *Proceedings of the Twenty-First International Conference on Machine Learning* (p. 26).
- Davis, J., & Goadrich, M. (2006). The Relationship between Precision-Recall and ROC Curves. *Proceedings of the 23rd International Conference on Machine Learning* (p. 233–240).
- Depersin, J., & Lecué, G. (2021). On the robustness to adversarial corruption and to heavy-tailed data of the Stahel-Donoho median of means. *preprint arXiv:2101.09117*.
- Falk, M. (1997). On Mad and Comedians. *Annals of the Institute of Statistical Mathematics*, 49(4), 615–644.
- Goldstein, M., & Dengel, A. (2012). Histogram-based outlier score (hbos): A fast unsupervised anomaly detection algorithm. *KI-2012: poster and demo track*, 9.
- Hinton, G.E., & Salakhutdinov, R. (2006). Reducing the Dimensionality of Data with Neural Networks. *Science*, 313, 504 - 507.
- Huang, Y., Jin, W., Yu, Z., Li, B. (2021). A robust anomaly detection algorithm based on principal component analysis. *Intelligent Data Analysis*, 25(2), 249–263.
- Hubert, M., Rousseeuw, P.J., Verdonck, T. (2010). *A DETERMINISTIC ALGORITHM FOR THE MCD* (Tech. Rep.). Celestijnenlaan 200B, B-3001 Leuven (Heverlee): Section of Statistics, Department of Mathematics, Katholieke Universiteit Leuven, The Netherlands.
- Jolliffe, I. (1986). *Principal Component Analysis*. New York: Springer.
- Kazempour, D., Hünemörder, M.A.X., Seidl, T. (2019). On comads and principal component analysis. *Similarity Search and Applications - 12th International Conference, SISAP 2019, Newark, NJ, USA, Proceedings* (pp. 273–280).
- Kriegel, H.-P., Kröger, P., Schubert, E., Zimek, A. (2008). A General Framework for Increasing the Robustness of PCA-Based Correlation Clustering Algorithms. *Proceedings of the 20th International Conference on Scientific and Statistical Database Management* (p. 418–435).
- Liu, F.T., Ting, K.M., Zhou, Z.-H. (2012). Isolation-Based Anomaly Detection. *ACM Transactions on Knowledge Discovery from Data*, 6(1).
- Maronna, R.A., & Yohai, V.J. (1995). The Behavior of the Stahel-Donoho Robust Multivariate Estimator. *Journal of the American Statistical*

- Association*, 90(429), 330-341.
- Moors, J.J.A. (1986). The meaning of kurtosis: Darlington reexamined. *The American Statistician*, 40(4), 283-284.
- Rousseeuw, P.J. (1984). Least median of squares regression. *Journal of the American Statistical Association*, 79(388), 871-880.
- Rousseeuw, P.J., & Driessen, K.V. (1999). A Fast Algorithm for the Minimum Covariance Determinant Estimator. *Technometrics*, 41(3), 212-223.
- Sajesh, T.A., & Srinivasan, M.R. (2012). Outlier detection for high dimensional data using the Comedian approach. *Journal of Statistical Computation and Simulation*, 82(5), 745-757.
- Shyu, M., Chen, S., Sarinnapakorn, K., Chang, L. (2003). A novel anomaly detection scheme based on principal component classifier. *in Proceedings of the IEEE Foundations and New Directions of Data Mining Workshop, in conjunction with the Third IEEE International Conference on Data Mining (ICDM'03)* (pp. 172-179).